

History-Aware Online Cache Placement in Fog-Assisted IoT Systems: An Integration of Learning and Control

Xin Gao, *Student Member, IEEE*, Xi Huang, *Member, IEEE*, Yinxu Tang, Ziyu Shao*, *Senior Member, IEEE*, Yang Yang, *Fellow, IEEE*

Abstract—In Fog-assisted IoT systems, it is a common practice to cache popular content at the network edge to achieve high quality of service. Due to uncertainties in practice such as unknown file popularities, cache placement scheme design is still an open problem with unresolved challenges: 1) how to maintain time-averaged storage costs under budgets, 2) how to incorporate online learning to aid cache placement to minimize performance loss (*a.k.a.* regret), and 3) how to exploit offline historical information to further reduce regret. In this paper, we formulate the cache placement problem with unknown file popularities as a constrained combinatorial multi-armed bandit (CMAB) problem. To solve the problem, we employ virtual queue techniques to manage time-averaged storage cost constraints, and adopt history-aware bandit learning methods to integrate offline historical information into the online learning procedure to handle the exploration-exploitation tradeoff. With an effective combination of online control and history-aware online learning, we devise a Cache Placement scheme with History-aware Bandit Learning called CPHBL. Our theoretical analysis and simulations show that CPHBL achieves a sublinear time-averaged regret bound. Moreover, the simulation results verify CPHBL’s advantage over the deep reinforcement learning based approach.

Index Terms—Internet of Things, proactive caching, fog computing, history-aware bandit learning, learning-aided online control.

I. INTRODUCTION

During recent years, the proliferation of *Internet of Things* (IoT) devices such as smart phones and the emerging of IoT applications such as video streaming have led to an unprecedented growth of data traffic [1]. To meet the explosively growing traffic demands at the network edge and facilitate IoT applications with high *quality of service* (QoS), caching popular contents at fog servers has emerged as a promising solution [2]–[5]. Figure 1 shows an example of wireless caching in a multi-tier Fog-assisted IoT system. As shown

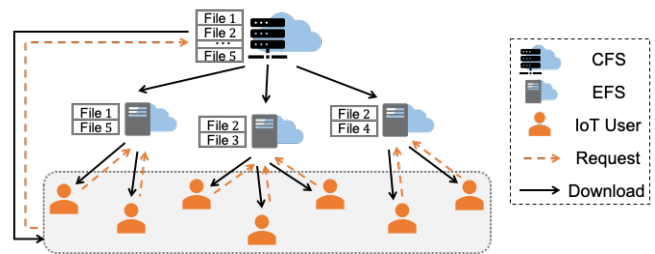


Fig. 1. An illustration of caching-enabled Fog-assisted IoT systems.

in the figure, by utilizing the storage resources on fog servers that are close to IoT devices, popular contents (*e.g.*, files) can be cached to achieve timely content delivery. Due to resource limit, each edge fog server (EFS) can cache only a subset of files to serve its associated IoT users. If a user’s requested file is found on the corresponding EFS (*a.k.a.* a *hit*), then it can be downloaded directly; otherwise, the file needs to be fetched from the central fog server (CFS) in the upper fog tier with extra bandwidth consumption and latency. Therefore, the key to maximize the benefits of caching in Fog-assisted IoT systems lies in the selection of a proper set of cached files (*a.k.a.* *cache placement*) on each EFS.

However, the effective design for cache placement remains as a challenging problem due to the uncertainty of file popularities in such systems. Specifically, as an important ingredient for cache placement optimization, file popularities are usually unknown in practice [6]. Such information can only be inferred implicitly from feedback information such as cache hit signals for user requests. Meanwhile, in practice, it is common for Fog-assisted IoT systems to retain offline historical observations (in terms of file request logs) on each EFS. Such offline information can also be exploited to estimate the file popularities in the procedure of cache placement. Nonetheless, it remains non-trivial about how to integrate both online feedback and offline historical information to reduce uncertainties in decision making and minimize the resulting performance loss (*a.k.a.* regret). If such an integration can be achieved, then each EFS can proactively update cache placement based on its learned popularity statistics to improve system performances.

Towards such a joint design, three challenges must be addressed. The first is concerning the tradeoff between conflicting performance metrics. On one hand, caching more popular

X. Gao is with the School of Information Science and Technology, ShanghaiTech University, Shanghai 201210, China, also with the Shanghai Institute of Microsystem and Information Technology, Chinese Academy of Sciences, Shanghai 200050, China, and with the University of Chinese Academy of Sciences, Beijing 100049, China. (E-mail: gaoxin@shanghaitech.edu.cn)

X. Huang, Y. Tang and Z. Shao are with the School of Information Science and Technology, ShanghaiTech University, Shanghai 201210, China. (E-mail: {huangxi, tangyx, shaozy}@shanghaitech.edu.cn)

Y. Yang is with Shanghai Institute of Fog Computing Technology (SHIFT), ShanghaiTech University, Shanghai 201210, China, and the Research Center for Network Communication, Peng Cheng Laboratory, Shenzhen 518000, China. (E-mail: yangyang@shanghaitech.edu.cn)

files on each EFS conduces to higher *cache hit rewards* (e.g., the total size of files served by wireless caching). On the other hand, the number of cached files should be limited to avoid excessive *storage costs* (e.g., memory footprint) [7]. Such a tradeoff between cache hit rewards and storage costs should be carefully considered for cache placement. The second is regarding the *exploration-exploitation* dilemma encountered in the online learning procedure; i.e., for each EFS, should it cache the files with empirically high estimated popularities (exploitation) or those files with inadequate feedback but potentially high popularities (exploration)? The third is about how to leverage offline historical information to further improve learning efficiency, which serves as a new degree of freedom in the design space of cache placement. Faced with such challenges, the interplays among online control, online learning, and offline historical information deserve a systematic investigation.

In this paper, we focus on the problem of proactive cache placement in caching-enabled Fog-assisted IoT systems with offline historical information and unknown file popularities under constraints on time-averaged storage costs of EFSs. We summarize our contributions and key results as follows.

- ◇ **Problem Formulation:** We formulate the problem as a stochastic optimization problem under uncertainties, with the aim to maximize the total cache hit reward in terms of the total size of files directly fetched from EFSs to IoT users over a finite time horizon. Meanwhile, we also consider the time-averaged storage cost constraint on each EFS. By exploiting the problem structure, we extend the settings of the recently developed bandit model [8] and reformulate the problem as a constrained combinatorial multi-armed bandit (CMAB) problem.
- ◇ **Algorithm Design:** To solve the formulated problem, we propose *CPHBL* (Cache Placement with History-aware Bandit Learning), a learning-aided cache placement scheme that conducts proactive and effective cache placement under time-averaged storage cost constraints. In general, CPHBL consists of two interacting procedures: the online learning procedure and the cache update procedure. Particularly, in the online learning procedure, we adopt the HUCB1 (UCB1 with Historic Data) method [9] to leverage both offline historical information and online feedback to learn the unknown file popularities with a decent exploration-exploitation tradeoff. In the cache update procedure, we leverage Lyapunov optimization method [10] to update cached files on EFSs in an adaptive manner, so that cache hit rewards can be maximized subject to the storage cost constraints.
- ◇ **Theoretical Analysis:** To the best of our knowledge, our work conducts the first systematic study on the integration of online control, online learning, and offline historical information. In particular, our theoretical analysis shows that our devised scheme achieves a near-optimal total cache hit reward under time-averaged storage cost constraints with a time-averaged regret bound of order $O(1/V + 1/T + \sqrt{(\log T)/(T + H_{\min})})$. Note that V is a positive tunable parameter, T is the length of time

horizon, and H_{\min} is the minimum number of offline historical observations among different EFSs.

- ◇ **Numerical Evaluation:** We conduct extensive simulations to investigate the performances of CPHBL and its variants. Moreover, we devise a novel deep reinforcement learning (DRL) based scheme as one of the baselines to be compared with CPHBL. Our simulation results not only verify our theoretical analysis, but also show the advantage of CPHBL over the baseline schemes.
- ◇ **New Degree of Freedom in the Design Space of Fog-Assisted IoT Systems:** We systematically investigate the fundamental benefits of offline historical information in Fog-assisted IoT systems. We provide both theoretical analysis and numerical simulations to evaluate such benefits. Our results reveal novel insights to system designers to improve their systems.

The rest of this paper is organized as follows. Section II discusses the related works. Section III illustrates our system model and problem formulation. Section IV shows our algorithm design, followed by the performance analysis in Section V. Section VI proposes a novel DRL based scheme as a baseline for evaluation and then Section VII discusses our simulation results. Finally, Section VIII concludes this paper.

II. RELATED WORK

In the past decades, cache placement has been widely studied to improve the performance of wireless networks such as IoT networks [20] and cellular networks [21]. Among existing works, those that are most relevant to our work are generally carried out from two perspectives: the *online control* perspective and the *online learning* perspective.

Online Control based Cache Placement: Most works that take the online control perspective formulated cache placement problems as stochastic network optimization problems with respect to different metrics. For example, in [7], Pang *et al.* jointly studied the cache placement and data sponsoring problems in mobile video content delivery networks. Their solution aimed to maximize the overall content delivery payoff with budget constraints on caching and delivery costs. Kwak *et al.* [11] devised a dynamic cache placement scheme to optimize service rates for user requests in a hierarchical wireless caching network. Wang *et al.* [12] developed a joint traffic forwarding and cache placement scheme to optimize the queuing delay and energy consumption of caching-enabled networks. In [13], Xu *et al.* proposed an online algorithm to jointly optimize wireless caching and task offloading with the goal of ultra-low task computation delays under a long-term energy constraint. In general, such works adopted Lyapunov optimization method [10] to solve their formulated problems through a series of per-time-slot adaptive control. Although the effectiveness of their solutions has been well justified, they generally assumed that file popularities or file requests are readily given prior to the cache placement procedure. Such assumptions are usually not the case in practice [6].

Online Learning based Cache Placement: Faced with constantly arriving file requests and unknown file popularities, a number of works adopted various learning techniques such

TABLE I. Comparison between our work and related works

	Optimization Metrics	Resource Constraints		Online Control	Online Learning	Offline History Information
		Per-time-slot Constraints	Long-term Constraints			
[7]	Revenue and cost of caching & delivery cost	•	•	•		
[11]	Service rates for file requests	•	•	•		
[12]	Queueing delay & energy consumption	•	•	•		
[13]	Task delay & energy consumption	•	•	•		
[14]	Cache hit reward	•			•	
[15]	Cache hit reward & file downloading cost	•			•	
[16]	Number of cache hits	•			•	
[17]	Weighted network utility	•			•	
[18]	Revenue of caching & content sharing cost	•			•	
[19]	Network transmission delay	•			•	
Our Work	Cache hit reward & storage cost	•	•	•	•	•

as deep learning [22]–[25], transfer learning [6] [26], and reinforcement learning [14]–[19], [27], [28] to improve the performance of wireless caching networks. However, existing solutions in such works cannot handle time-averaged constraints. Besides, they mainly resorted to time-consuming offline pre-training and heuristic hyper-parameter tuning to produce their solutions. Moreover, they generally provided no theoretical guarantee but limited insights for the resulting performance.

Bandit learning is another method that is widely adopted to promote the performance of such systems. So far, it has been applied to solve scheduling problems such as task offloading [29], task allocation [30], and path selection [31]. The most relevant to our work are those which consider optimizing proactive cache placement in terms of different performance metrics. For example, Blasco *et al.* [14] [15] studied the cache placement problem for a single caching unit with multiple users. By considering the problem as a CMAB problem, in [14] they aimed to maximize the amount of served traffic through wireless caching, while in [15] they further took file downloading costs into the account for optimization. In [16], Müller *et al.* proposed a cache placement scheme based on contextual bandits, which learns the context-dependent content popularity to maximize the number of cache hits. Zhang *et al.* [17] studied the network utility maximization problem in the context of cache placement with a non-fixed content library over time. Song *et al.* [18] proposed a joint cache placement and content sharing scheme among cooperative caching units to maximize the content caching revenue and minimize the content sharing expense. In [19], Xu *et al.* modeled the procedure of cache placement with multiple caching units from the perspective of multi-agent multi-armed bandit (MAMAB) and devised an online scheme to minimize the accumulated transmission delay over time. Such works generally do not consider the storage costs on EFSs in terms of memory footprint. In practice, without such a consideration, caching files with excessively high storage costs may offset the benefits of wireless caching. Moreover, none of such works exploits offline historical information in their learning procedures.

Novelty of Our Work: Different from existing works, to our best knowledge, our work presents the first systematic study on the synergy of online control, online learning, and offline historical information. In particular, we conduct theoretical analysis to characterize the joint impacts of online control, online learning, and offline information on the performances

TABLE II. Key notations

Notation	Description
T	Length of time horizon
\mathcal{N}	Set of EFSs with $ \mathcal{N} \triangleq N$
\mathcal{K}	Set of IoT users with $ \mathcal{K} \triangleq K$
\mathcal{K}_n	Set of IoT users served by EFS n
\mathcal{F}	Set of files with $ \mathcal{F} \triangleq F$
L_f	Size of file f
M_n	Storage capacity of EFS n
$\theta_{k,f}(t)$	Indicator of whether file f is requested by IoT user k in time slot t
$D_{n,f}(t)$	Total number of IoT users in set \mathcal{K}_n who request for file f in time slot t
$d_{n,f}$	Popularity of file f on EFS n , $d_{n,f} \triangleq \mathbb{E}[D_{n,f}(t)]$
$H_{n,f}$	Number of offline historical observations with respect to the popularity of file f on EFS n
$D_{n,f}^h(s)$	Total number of IoT users in set \mathcal{K}_n who request for file f according to the s -th offline historical observation
$\tilde{d}_{n,f}(t)$	Estimated popularity of file f on EFS n in time slot t
$X_{n,f}(t)$	Cache placement decision for caching file f on EFS n in time slot t
$C_n(t)$	Storage cost of EFS n in time slot t
$R_{n,f}(t)$	Cache hit reward of EFS n with respect to file f in time slot t
$R_n(t)$	Total cache hit reward of EFS n in time slot t
b_n	Storage cost budget for EFS n

of cache placement. Our results also provide novel insights to the designers of Fog-assisted IoT systems. The comparison between our work and existing works is presented in Table I.

III. SYSTEM MODEL AND PROBLEM FORMULATION

In this section, we describe our system model in detail. Then we present our problem formulations. Key notations in this paper are summarized in Table II.

A. Basic Model

We consider a caching-enabled Fog-assisted IoT system that operates over a finite time horizon of T time slots. In the system, there is a central fog server (CFS) that manages N edge fog servers (EFSs) to serve K IoT users. The fog servers and IoT users communicate with each other through wireless connections. We assume that OFDM (orthogonal frequency

division multiplexing) [32] is employed as the underlying wireless transmission mechanism. Under such a mechanism, the co-channel interference among fog servers and IoT users can be eliminated by the orthogonal subcarrier allocation. Based on such an assumption, we abstract the physical-layer wireless links as bit pipes and focus on the network-layer data communications between servers and IoT users. We denote the sets of EFSs and users by $\mathcal{N} \triangleq \{1, 2, \dots, N\}$ and $\mathcal{K} \triangleq \{1, 2, \dots, K\}$, respectively. For each EFS n , we define \mathcal{K}_n ($\mathcal{K}_n \subseteq \mathcal{K}$, $|\mathcal{K}_n| = K_n$) as the set of IoT users within its service range. Note that each IoT user is served by one and only one EFS and thus the sets $\{\mathcal{K}_n\}_n$ are disjoint.

Particularly, we focus on the scenario in which IoT users request to download files from EFSs. We assume that the CFS has stored all of F files (denoted by set $\mathcal{F} \triangleq \{1, 2, \dots, F\}$) that could be requested within the time horizon. Each file f has a fixed size of L_f storage units. Due to caching capacity limit, each EFS n only has M_n units of storage to cache a portion of the files and $M_n < \sum_{f \in \mathcal{F}} L_f$. Accordingly, if a user cannot find its requested file on its associated EFS, it will request to download the file directly from the CFS. We assume that the CFS can provide simultaneous and independent file deliveries to all EFSs and IoT users. An example which illustrates our system model is shown in Figure 1.

B. File Popularity

On each EFS n , we consider the popularity of each file f as the expected number of users to request file f per time slot, whose ground-truth value is denoted by $d_{n,f}$. We assume that each file's popularity remains constant within the time horizon. In practice, such file popularities are usually unknown *a priori* and can only be inferred based on online feedback information collected after user requests have been served.

Next, we introduce some variables to characterize user dynamics with respect to file popularity. We define binary variable $\theta_{k,f}(t) \in \{0, 1\}$ such that $\theta_{k,f}(t) = 1$ if IoT user k requests for file f in time slot t and $\theta_{k,f}(t) = 0$ otherwise. Then we denote the file requests of IoT user k during time slot t by vector $\boldsymbol{\theta}_k(t) \triangleq (\theta_{k,1}(t), \theta_{k,2}(t), \dots, \theta_{k,F}(t))$. Meanwhile, we use $D_{n,f}(t) \triangleq \sum_{k \in \mathcal{K}_n} \theta_{k,f}(t)$ to denote the total number of IoT users in set \mathcal{K}_n who request for file f on EFS n in time slot t . Note that $D_{n,f}(t)$ is a discrete random variable over a support set $\{0, 1, \dots, K_n\}$ and assumed to be *i.i.d.* across time slots with a mean of $d_{n,f}$.

Besides, we assume that initially (*i.e.*, $t = 0$), each EFS is provided with a fixed set of offline historical observations with respect to the number of requests for each file. Specifically, the offline historical observations for file f on EFS n are denoted by $\{D_{n,f}^h(0), D_{n,f}^h(1), \dots, D_{n,f}^h(H_{n,f} - 1)\}$, where we define $H_{n,f} \geq 0$ as the number of offline historical observations about file f on EFS n . When $H_{n,f} = 0$, there is no offline historical information. Let $D_{n,f}^h(s)$ denote the s -th offline historical observation. Here we use superscript h to indicate that $D_{n,f}^h(s)$ belongs to offline historical information. Note that such observations are given as prior information when $t = 0$. Their values are assumed to follow the same distribution as the file popularities over the time horizon.

C. System Workflow

During each time slot t , the system operates across two phases: the caching phase and the service phase.

- ◇ *Caching phase*: At the beginning of time slot t , each EFS n updates its cached files and consumes a storage cost for each cached file. Then each EFS n broadcasts its cache placement to all IoT users in set \mathcal{K}_n .
- ◇ *Service phase*: Each IoT user generates file requests. For each request, if it is not cached on the EFS, then the user will fetch the file from the CFS. Otherwise, the user directly downloads the file from the EFS and the EFS will receive a corresponding cache hit reward.

In the next few subsections, we present the definitions of cache placement decisions, storage costs, and cache hit rewards, respectively.

D. Cache Placement Decision

For each EFS n , we denote its cache placement decision made during each time slot t by a binary vector $\mathbf{X}_n(t) \triangleq (X_{n,1}(t), X_{n,2}(t), \dots, X_{n,F}(t))$. Each entry $X_{n,f}(t) = 1$ if EFS n decides to cache file f during time slot t and $X_{n,f}(t) = 0$ otherwise. Note that the total size of cached files on EFS n does not exceed its storage capacity, *i.e.*,

$$\sum_{f \in \mathcal{F}} L_f X_{n,f}(t) \leq M_n, \quad \forall n \in \mathcal{N}, t. \quad (1)$$

E. Storage Cost

For each EFS n , caching file f during a time slot t will incur a storage cost of αL_f , where $\alpha > 0$ is the unit storage cost. The storage cost can be viewed as the memory footprint for maintaining the file which is proportional to the size of file f . Accordingly, given decision $\mathbf{X}_n(t)$, we define the total storage cost on EFS n during time slot t as

$$C_n(t) \triangleq \sum_{f \in \mathcal{F}} \alpha L_f X_{n,f}(t). \quad (2)$$

F. Cache Hit Reward

Recall that during each time slot t , for *each* requested file f , if $X_{n,f}(t) = 1$, then EFS n will receive a reward L_f for the corresponding cache hit [14] (in terms of amounts of traffic to fetch file f from EFS n). Then given the cache placement $\mathbf{X}_n(t)$ and user demand $D_{n,f}(t)$ during time slot t , we define the cache hit reward of EFS n with respect to file f as

$$R_{n,f}(t) \triangleq L_f D_{n,f}(t) X_{n,f}(t). \quad (3)$$

Note that the cache hit reward $R_{n,f}(t) = 0$ if file f is not cached on EFS n during time slot t (*i.e.*, $X_{n,f}(t) = 0$). Accordingly, we define the total cache hit reward of EFS n during time slot t as

$$R_n(t) = \hat{R}_n(\mathbf{X}_n(t)) \triangleq \sum_{f \in \mathcal{F}} L_f D_{n,f}(t) X_{n,f}(t). \quad (4)$$

G. Problem Formulation

To achieve effective cache placement with a high QoS, two goals are considered in our work. One is to maximize the total size of transmitted files from all EFSs so that requests from IoT users can obtain timely services. In our model, this is equivalent to maximizing the time-averaged cache hit reward of all EFSs over a time horizon of T time slots. The other is to guarantee a budgeted usage of storage costs over time. To this end, for each EFS n , we first define b_n as the storage cost budget for caching files. Then we impose the following constraint to ensure the time-averaged storage costs under the budget in the long run:

$$\limsup_{t \rightarrow \infty} \frac{1}{t} \sum_{\tau=0}^{t-1} \mathbb{E}[C_n(\tau)] \leq b_n, \forall n \in \mathcal{N}. \quad (5)$$

Based on the above system model and constraints, our problem formulation is given by

$$\text{maximize}_{\{\mathbf{X}(t)\}_t} \frac{1}{T} \sum_{t=0}^{T-1} \sum_{n \in \mathcal{N}} \mathbb{E}[R_n(t)] \quad (6a)$$

$$\text{subject to } X_{n,f}(t) \in \{0, 1\}, \forall n \in \mathcal{N}, f \in \mathcal{F}, t, \quad (6b)$$

(1), (5).

In the above formulation, the objective (6a) is to maximize the time-averaged expectation of total cache hit reward of all EFSs. Constraint (6b) states that each cache placement decision $X_{n,f}(t)$ should be a binary variable. The constraint in (1) guarantees that the total size of cached files on each EFS should not exceed the storage capacity. The constraint in (5) ensures the budget constraint on the storage cost of each EFS.

IV. ALGORITHM DESIGN

For problem (6), given the full knowledge of user demands $\{D_{n,f}(t)\}_{n,f}$, it can be solved asymptotically optimally by Lyapunov optimization methods [10]. However, file popularities are usually not given as prior information in practice. Faced with such uncertainties, online learning needs to be incorporated to guide the decision-making process by estimating the statistics of file popularities from both online feedback and offline historical information. To this end, we need to deal with the well-known *exploration-exploitation* dilemma, *i.e.*, how to balance the decisions made to acquire new knowledge about file popularity to improve learning accuracy (*exploration*) and the decisions made to leverage current knowledge to select the empirically most popular files (*exploitation*). For such a decision-making problem under uncertainty, we consider it through the lens of combinatorial multi-armed bandit (CMAB) with extended settings. With an effective integration of online bandit learning, online control, and offline historical information, we devise a history-aware learning-aided cache placement scheme called CPHBL (Cache Placement with History-aware Bandit Learning) to solve problem (6). Figure 2 depicts the design of CPHBL. During each time slot, under CPHBL, each EFS first estimates the popularity of different files based on both offline historical information and collected online feedback. Based on such estimates, the EFS determines and

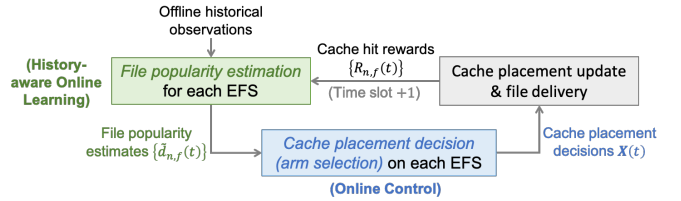


Fig. 2. An illustration of our algorithm design.

updates its cache placement in the current time slot. After the update, each EFS delivers requested cached files to IoT users. For each cache hit, a reward will be credited to the EFS.

In the following subsections, we extend the settings of the existing CMAB model and demonstrate the reformulation of problem (6) under such settings. Then we articulate our algorithm design with respect to online learning and online control procedures, respectively. Finally, we discuss the computational complexity of our devised algorithm.

A. Problem Reformulation

The basic settings of CMAB [33] consider a sequential interaction between a player and its environment with multiple actions (*a.k.a.* arms) over a finite number of rounds. During each round, the player selects a subset of available arms to play. For each selected arm, the agent will receive a reward that is sampled from an unknown distribution. The overall goal of the player is to find an effective arm-selection scheme to maximize its expected cumulative reward.

Based on the CMAB model, Li *et al.* [8] extended the settings of classical CMAB by allowing the temporary unavailability of arms while considering the fairness of arm selection. Inspired by their work, we reformulate problem (6) as a constrained CMAB problem in the following way. We view each EFS as a distinct player and each file as an arm. During each time slot t , each player $n \in \mathcal{N}$ selects a subset of arms to play. If player n chooses to play arm $f \in \mathcal{F}$ in time slot t , then file f will be cached on EFS n and a reward $R_{n,f}(t) = L_f D_{n,f}(t)$ will be received by the player. Recall that the file demand $D_{n,f}(t)$ during each time slot t is a random variable with an unknown mean $d_{n,f}$ and is *i.i.d.* across time slots. Accordingly, reward $R_{n,f}(t)$ is also an *i.i.d.* random variable with an unknown mean $r_{n,f} = \mathbb{E}[R_{n,f}(t)] = L_f d_{n,f}$. Meanwhile, the cache placement decision $\mathbf{X}_n(t) = (X_{n,1}(t), X_{n,2}(t), \dots, X_{n,F}(t))$ of EFS n corresponds to the arm selection of player n in time slot t . Specifically, $X_{n,f}(t) = 1$ if arm f is chosen and $X_{n,f}(t) = 0$ otherwise. Our goal is to devise an arm selection scheme for the players to maximize their expected cumulative rewards subject to the constraints in (1) and (5).

Remark: Our model extends the settings of the bandit model proposed by [8] in the following four aspects. First, we consider multiple players instead of one player. Second, the storage cost constraints in our problem are more challenging to handle than the arm fairness constraints in [8]. Specifically, under our settings, the selection of each arm for a player is coupled together under storage cost constraints, whereas in [8] there is no such coupling among arm selections. Third, we

consider the storage capacity constraint for each player during each time slot, which is ignored in [8]. Last but not least, we consider a more general reward function with respect to file uncertainties. The above extensions make our reformulated problem more challenging than the problem in [8].

To characterize the performance loss (*a.k.a.* regret) due to decision making under such uncertainties, we define the regret with respect to a given scheme (denoted by decision sequence $\{\mathbf{X}(t)\}_t$) as

$$Reg(T) \triangleq R^* - \frac{1}{T} \sum_{t=0}^{T-1} \sum_{n \in \mathcal{N}} \mathbb{E} \left[\hat{R}_n(\mathbf{X}_n(t)) \right], \quad (7)$$

where constant R^* is defined as the optimal time-averaged total expected reward for all players. In fact, maximizing the time-averaged expected reward is equivalent to minimizing the regret. Therefore, we can rewrite problem (6) as follows:

$$\underset{\{\mathbf{X}(t)\}_t}{\text{minimize}} \quad Reg(T) \quad (8a)$$

$$\text{subject to} \quad (1)(5)(6b). \quad (8b)$$

To solve problem (8), we integrate history-aware bandit learning methods and virtual queue techniques to handle the exploration-exploitation tradeoff and the time-averaged storage cost constraints, respectively. In the following subsections, we demonstrate our algorithm design in detail.

B. Online Bandit Learning with Offline Historical Information

By (4), the regret defined in (7) can be rewritten as

$$\begin{aligned} Reg(T) &= R^* - \frac{1}{T} \sum_{t=0}^{T-1} \sum_{n \in \mathcal{N}} \sum_{f \in \mathcal{F}} L_f \mathbb{E} [D_{n,f}(t) X_{n,f}(t)] \\ &= R^* - \frac{1}{T} \sum_{t=0}^{T-1} \sum_{n \in \mathcal{N}} \sum_{f \in \mathcal{F}} L_f d_{n,f} \mathbb{E} [X_{n,f}(t)], \end{aligned} \quad (9)$$

where the last equality holds due to the independence between user demand $D_{n,f}(t)$ and cache placement $X_{n,f}(t)$, and the fact that $\mathbb{E}[D_{n,f}(t)] = d_{n,f}$. By (9) and our previous analysis, to solve problem (8), each EFS n should learn the unknown file popularity $d_{n,f}$ with respect to each file f .

During each time slot t , after updating cached files according to decision $\mathbf{X}_n(t)$, each EFS n observes the current demand $D_{n,f}(t)$ for each cached file f . Then EFS n transmits requested files to IoT users and acquires cache hit rewards. Based on the pre-given offline historical information and cache hit feedback from IoT users, we have the following estimate for each file popularity $d_{n,f}$:

$$\tilde{d}_{n,f}(t) = \min \left\{ \bar{d}_{n,f}(t) + K_n \sqrt{\frac{3 \log t}{2(h_{n,f}(t) + H_{n,f})}}, K_n \right\}. \quad (10)$$

In (10), $\bar{d}_{n,f}(t)$ is the empirical mean of the number of requests for file f that involves both offline historical observations and collected online feedbacks; $h_{n,f}(t)$ counts the number of time slots (within the first t time slots) during which file f is chosen to be cached on EFS n ; and K_n denotes the number of users served by EFS n . Specifically, the number of

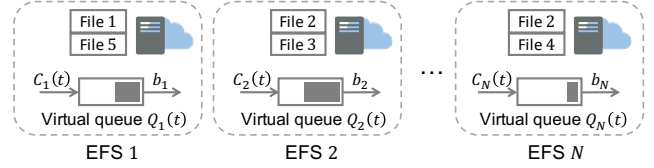


Fig. 3. An illustration of virtual queues for storage cost on each EFS. Each EFS $n \in \mathcal{N}$ maintains a virtual queue $Q_n(t)$ with an input of $C_n(t)$ and an output of b_n during each time slot t . If the queuing process $\{Q_n(t)\}_t$ is strongly stable, then the time-averaged storage cost constraint (5) on EFS n can be satisfied.

observations $h_{n,f}(t)$ and the empirical mean of file popularity $\bar{d}_{n,f}(t)$ by time slot t are defined as follows, respectively:

$$h_{n,f}(t) \triangleq \sum_{\tau=0}^{t-1} X_{n,f}(\tau), \quad (11)$$

$$\bar{d}_{n,f}(t) \triangleq \frac{\sum_{\tau=0}^{t-1} D_{n,f}(\tau) X_{n,f}(\tau) + \sum_{s=0}^{H_{n,f}-1} D_{n,f}^h(s)}{h_{n,f}(t) + H_{n,f}}. \quad (12)$$

Remark: In (10), the term $K_n \sqrt{\frac{3 \log t}{2(h_{n,f}(t) + H_{n,f})}}$ denotes the *confidence radius* [34] that represents the degree of uncertainty with respect to the empirical estimate $\bar{d}_{n,f}(t)$. The larger the confidence radius, the greater the value of the estimate (10) and thus the greater the chance for file f to be cached on EFS n . In the confidence radius, the term $h_{n,f}(t) + H_{n,f}$ is the total number of observations (including both online observations and offline historical observations) for the popularity of file f on EFS n . Given a small number of observations (*i.e.*, $h_{n,f}(t) + H_{n,f} \ll t$), the confidence radius for the empirical estimate $\bar{d}_{n,f}(t)$ will be large, which implies that the file is rarely cached and hence a great uncertainty about the estimate. In this case, the confidence radius plays a dominant role in the estimate $\tilde{d}_{n,f}(t)$. As a result, file f will be more likely to be cached on EFS n . In contrast, if a file has been cached for an adequate number of times, its popularity estimate (10) will be close to its empirical mean and the role of confidence radius will be marginalized. Besides, the estimate (10) also characterizes the effects of offline historical information and online feedback information. Particularly, in the early stage (when t is small), suppose that the number of online observations is much smaller than the number of offline historical observations, *i.e.*, $h_{n,f}(t) \ll H_{n,f}$. In this case, the estimate (10) mainly depends on offline historical information. However, as more and more online feedbacks are collected, the impact of online information becomes more dominant.

C. Storage Cost Budgets with Virtual Queue Technique

By leveraging Lyapunov optimization techniques [10], we transform the time-averaged storage cost constraints into queue stability constraints. Specifically, we introduce a virtual queue $Q_n(t)$ for each EFS $n \in \mathcal{N}$ with $Q_n(0) = 0$ to handle the time-averaged constraints (5) on storage costs. As illustrated in Figure 3, each virtual queue $Q_n(t)$ is updated during each time slot t as follows:

$$Q_n(t+1) = [Q_n(t) - b_n]^+ + C_n(t), \quad (13)$$

in which we define $[\cdot]^+ \triangleq \max\{\cdot, 0\}$. Note that the constraints in (5) are satisfied only when the queueing process $\{Q_n(t)\}_t$ for each EFS n is strongly stable [10]. Intuitively, the mean queue inputs (*i.e.*, storage costs) should not be greater than the mean queue outputs (*i.e.*, cost budgets). Otherwise, virtual queues will be overloaded, thereby violating the constraints in (5). To maintain the stability of virtual queues and minimize the regret, we transform problem (8) into a series of per-time-slot subproblems. We show the detailed derivation in Appendix A. Specifically, during each time slot t , we aim to solve the following problem for each EFS $n \in \mathcal{N}$:

$$\underset{\mathbf{X}_n(t)}{\text{maximize}} \quad \sum_{f \in \mathcal{F}} \tilde{w}_{n,f}(t) X_{n,f}(t) \quad (14a)$$

$$\text{subject to} \quad \sum_{f \in \mathcal{F}} L_f X_{n,f}(t) \leq M_n, \quad (14b)$$

$$X_{n,f}(t) \in \{0, 1\}, \forall f \in \mathcal{F}, \quad (14c)$$

where $\tilde{w}_{n,f}(t)$ is defined as

$$\tilde{w}_{n,f}(t) \triangleq L_f (V \tilde{d}_{n,f}(t) - \alpha Q_n(t)). \quad (15)$$

In (15), parameter V is a tunable positive constant; weight $\tilde{w}_{n,f}(t)$ can be viewed as the gain of caching file f on EFS n during time slot t ; and the objective of problem (14) is to maximize the total gain of caching files on EFS n under the storage capacity constraint in (14b).

During each time slot t , we solve problem (14) for each EFS n to determine its cache placement $\mathbf{X}_n(t)$. We split set \mathcal{F} into two disjoint sets $\mathcal{F}_{n,1}(t) = \{f \in \mathcal{F} : \tilde{w}_{n,f}(t) \geq 0\}$ and $\mathcal{F}_{n,2}(t) = \{f \in \mathcal{F} : \tilde{w}_{n,f}(t) < 0\}$ for each EFS n . Specifically, for each file $f \in \mathcal{F}$,

- 1) if $\tilde{d}_{n,f}(t) \geq \alpha Q_n(t)/V$, then $\tilde{w}_{n,f}(t) \geq 0$ and $f \in \mathcal{F}_{n,1}(t)$;
- 2) if $\tilde{d}_{n,f}(t) < \alpha Q_n(t)/V$, then $\tilde{w}_{n,f}(t) < 0$ and $f \in \mathcal{F}_{n,2}(t)$.

For each file $f \in \mathcal{F}_{n,2}(t)$, the corresponding optimal placement decision is $X_{n,f}(t) = 0$ since caching file f on EFS n will incur a negative gain, *i.e.*, $\tilde{w}_{n,f}(t) < 0$. By setting $X_{n,f}(t) = 0$ for each file $f \in \mathcal{F}_{n,2}(t)$, we can regard problem (14) as a classical Knapsack problem [35]

$$\begin{aligned} & \underset{\{X_{n,f}(t)\}_{f \in \mathcal{F}_{n,1}(t)}}{\text{maximize}} && \sum_{f \in \mathcal{F}_{n,1}(t)} \tilde{w}_{n,f}(t) X_{n,f}(t) \\ & \text{subject to} && \sum_{f \in \mathcal{F}_{n,1}(t)} L_f X_{n,f}(t) \leq M_n, \\ & && X_{n,f}(t) \in \{0, 1\}, \forall f \in \mathcal{F}_{n,1}(t). \end{aligned} \quad (16)$$

Intuitively, from the lens of Knapsack problem, we have a number of items (files) in set $\mathcal{F}_{n,1}(t)$ and a knapsack (EFS n 's cache) with a capacity of M_n . The weight of each item $f \in \mathcal{F}_{n,1}(t)$ is L_f , while the value of putting item f in the knapsack is $\tilde{w}_{n,f}(t)$. Given the weights and values of all items, our goal is to select and put a subset of the items from $\mathcal{F}_{n,1}(t)$ into the knapsack with the maximum total value. Such a problem can be solved optimally by applying dynamic programming (DP) algorithm [36].

D. Integrated Algorithm Design

Based on the design presented in the previous two subsections, we propose a novel learning-aided proactive cache placement scheme called CPHBL (Cache Placement with History-aware Bandit Learning). The pseudocode of CPHBL is presented in Algorithm 1. In particular, we denote the file indices in set $\mathcal{F}_{n,1}(t)$ by $\phi_{n,1}(t), \phi_{n,2}(t), \dots, \phi_{n,|\mathcal{F}_{n,1}(t)|}(t)$, respectively. We use $v(i, m)$ to denote the optimal value of problem (16) when only the first i files (*i.e.*, files indexed by $\phi_{n,1}(t), \dots, \phi_{n,i}(t)$) in $\mathcal{F}_{n,1}(t)$ can be selected to store in the remaining memory capacity of m storage units. Regarding CPHBL, we have the following remarks.

Remark 1: In (15), the value of parameter V in weight $\tilde{w}_{n,f}(t)$ measures the relative importance of achieving high cache hit rewards to ensuring storage cost constraints. Note that the value of $\tilde{w}_{n,f}(t)$ is positively proportional to the value of parameter V . Therefore, for each file $f \in \mathcal{F}$, the gain $\tilde{w}_{n,f}(t)$ of caching file f on EFS n during time slot t will increase as the value of V increases. Under CPHBL, EFS n will cache more files to achieve not only a higher gain but also a larger storage cost. Moreover, files with high estimated mean cache hit rewards would be the first to be cached.

Remark 2: To ensure the storage cost constraints in (5), CPHBL would restrict each EFS to cache limited files as its virtual queue backlog size becomes large. Intuitively, for each EFS n , if its time-averaged storage cost tends to exceed the cost budget b_n , its corresponding virtual queue backlog size $Q_n(t)$ will be large. By the definition of weight $\tilde{w}_{n,f}(t)$ in (15), the value of $\tilde{w}_{n,f}(t)$ is negatively proportional to the virtual queue backlog size $Q_n(t)$. Therefore, when the value of $Q_n(t)$ increases, the weight $\tilde{w}_{n,f}(t)$ of caching file f on EFS n tends to be negative. Under CPHBL, files with negative weights will not be cached, which conduces to a low time-averaged storage cost.

E. Computational Complexity of CPHBL

The computational complexity of CPHBL mainly lies in the decision making for cache placement on each EFS $n \in \mathcal{N}$ (line 8 in Algorithm 1). In this process, DP is adopted to solve problem (14) with a computational complexity of $O(FM_n)$ [36]. Note that F denotes the total number of files on the CFS and M_n denotes the storage capacity of EFS n . In practice, the cache placement procedure can be implemented in a distributed fashion over EFNs; accordingly, the total computational complexity of CPHBL is $O(F \max_{n \in \mathcal{N}} M_n)$.

V. PERFORMANCE ANALYSIS

For each EFS n , given the number K_n of its served users and its storage capacity M_n , as well as the size L_f of each file $f \in \mathcal{F}$, we establish the following two theorems to characterize the performance of CPHBL.

A. Storage Cost Constraints

A budget vector $\mathbf{b} = (b_1, b_2, \dots, b_N)$ of storage costs is said to be *feasible* if there exists a feasible cache placement scheme under which all storage cost constraints in (5) can be

Algorithm 1 Cache Placement with History-aware Bandit Learning (CPHBL)

```

1: Initialize  $h_{n,f}(0) = 0$ ,  $\tilde{d}_{n,f}(0) = \frac{1}{H_{n,f}} \sum_{s=0}^{H_{n,f}-1} D_{n,f}^h(s)$  and
 $\tilde{d}_{n,f}(0) = K_n$  for each EFS  $n \in \mathcal{N}$  and each file  $f \in \mathcal{F}$ . In
each time slot  $t \in \{0, 1, \dots\}$ :
  %History-aware Online Learning
2: for each EFS  $n \in \mathcal{N}$  and each file  $f \in \mathcal{F}$  do
3:   if  $h_{n,f}(t) + H_{n,f} > 0$  and  $t > 0$  then
4:      $\tilde{d}_{n,f}(t) \leftarrow \min \left\{ \tilde{d}_{n,f}(t) + K_n \sqrt{\frac{3 \log t}{2(h_{n,f}(t) + H_{n,f})}}, K_n \right\}$ .
5:   end if
6: end for
  %Cache Placement
7: for each EFS  $n \in \mathcal{N}$  do
8:   SETCACHEPLACEMENT( $t, n, \{\tilde{d}_{n,f}(t)\}_f$ ).
9: end for
  %Update of Statistics and Virtual Queues
10: Update cached files according to  $\mathbf{X}(t)$  and virtual queues  $\mathbf{Q}(t)$ 
according to (13).
11: for each EFS  $n \in \mathcal{N}$  and each file  $f \in \mathcal{F}$  do
12:    $h_{n,f}(t+1) \leftarrow h_{n,f}(t) + X_{n,f}(t)$ .
13:    $\tilde{d}_{n,f}(t+1) \leftarrow \frac{h_{n,f}(t) + H_{n,f}}{h_{n,f}(t+1) + H_{n,f}} \tilde{d}_{n,f}(t) + \frac{D_{n,f}(t) X_{n,f}(t)}{h_{n,f}(t+1) + H_{n,f}}$ .
14: end for

```

```

1: function SETCACHEPLACEMENT( $t, n, \{\tilde{d}_{n,f}(t)\}_f$ )
2: Inputs: At the beginning of time slot  $t$ , for EFS  $n$ , given file
demand estimate  $\{\tilde{d}_{n,f}(t)\}_f$ .
3: Set  $\mathcal{F}_{n,1}(t) \leftarrow \emptyset$ .
4: for each file  $f \in \mathcal{F}$  do
5:   Set  $\tilde{w}_{n,f}(t) \leftarrow L_f(V\tilde{d}_{n,f}(t) - Q_n(t))$ .
6:   if  $\tilde{w}_{n,f}(t) < 0$  then
7:     Set  $X_{n,f}(t) \leftarrow 0$ .
8:   else
9:     Set  $\mathcal{F}_{n,1}(t) \leftarrow \mathcal{F}_{n,1}(t) \cup \{f\}$ .
10:  end if
11: end for
12: Initialize  $v_n(i, m) = 0$  for  $i \in \{0, 1, 2, \dots, |\mathcal{F}_{n,1}(t)|\}$  and
 $m \in \{0, 1, \dots, M_n\}$ .
13: for each  $i \in \{1, 2, \dots, |\mathcal{F}_{n,1}(t)|\}$  do
14:   for each  $m \in \{1, \dots, M_n\}$  do
15:     if  $L_{\phi_{n,i}(t)} > m$  then
16:       Set  $v_n(i, m) \leftarrow v_n(i-1, m)$ .
17:     else
18:       Set  $v_n(i, m) \leftarrow \max \{v_n(i-1, m), v_n(i-1, m -
L_{\phi_{n,i}(t)} + \tilde{w}_{n,\phi_{n,i}(t)}(t))\}$ .
19:     end if
20:   end for
21: end for
22: SETOPTPLACEMENT( $n, |\mathcal{F}_{n,1}(t)|, M_n$ ).
23: end function

```

satisfied. We define the set of all feasible budget vectors as the *maximal feasibility region* of the system, which is denoted by the set \mathcal{B} . The following theorem shows that all virtual queues are strongly stable under CPHBL when \mathbf{b} is an interior point of \mathcal{B} .

Theorem 1: Suppose that the budget vector \mathbf{b} lies in the interior of \mathcal{B} , then the time-averaged storage cost constraints in (5) are satisfied under CPHBL. Moreover, the virtual queues defined in (13) are strongly stable and there exists some

```

1: function SETOPTPLACEMENT( $n, i, m$ )
2: Inputs: For EFS  $n$ , given the number of files  $i$  and the
remaining storage size  $m$ .
3: if  $i \geq 1$  then
4:   if  $v_n(i, m) = v_n(i-1, m - L_{\phi_{n,i}(t)} + \tilde{w}_{n,\phi_{n,i}(t)}(t))$  and
 $m - L_{\phi_{n,i}(t)} \geq 0$  then
5:     Set  $X_{n,\phi_{n,i}(t)}(t) \leftarrow 1$ .
6:     SETOPTPLACEMENT( $n, i-1, m - L_{\phi_{n,i}(t)}$ ).
7:   else if  $v_n(i, m) = v_n(i-1, m)$  then
8:     Set  $X_{n,\phi_{n,i}(t)}(t) \leftarrow 0$ .
9:     SETOPTPLACEMENT( $n, i-1, m$ ).
10:  end if
11: end if
12: end function

```

constant $\epsilon > 0$ such that

$$\limsup_{t \rightarrow \infty} \frac{1}{t} \sum_{\tau=0}^{t-1} \sum_{n \in \mathcal{N}} \mathbb{E}[Q_n(\tau)] \leq \frac{B + V \sum_{n \in \mathcal{N}} 2K_n M_n}{\epsilon}, \quad (17)$$

where $B \triangleq \sum_{n \in \mathcal{N}} (b_n^2 + \alpha^2 M_n^2) / 2$.

The proof of Theorem 1 is given in Appendix B.

Remark 1: Theorem 1 shows that CPHBL ensures the stability of virtual queue backlogs $\{Q_n(t)\}_n$. Moreover, the time-averaged total backlog size of such virtual queues is linearly proportional to the value of parameter V . In other words, given that vector \mathbf{b} is interior to the maximal feasibility region, under CPHBL, the time-averaged total storage cost is tunable and guaranteed to be under the given budget.

B. Regret Bound

Our second theorem provides an upper bound for the regret incurred by CPHBL over time.

Theorem 2: Under CPHBL, the regret (7) over time horizon T is upper bounded as follows:

$$\text{Reg}(T) \leq \frac{B}{V} + \frac{4 \sum_{n \in \mathcal{N}} K_n M_n}{T} + \Gamma \sqrt{\frac{\log T}{T + H_{\min}}}, \quad (18)$$

in which we define the constants $B \triangleq \sum_{n \in \mathcal{N}} (b_n^2 + \alpha^2 M_n^2) / 2$ and $\Gamma \triangleq 2 \sum_{n \in \mathcal{N}} K_n \sqrt{6M_n \sum_{f \in \mathcal{F}} L_f}$. Here T is the time horizon length and $H_{\min} \triangleq \min_{n,f} H_{n,f}$ is the the minimal number of offline historical observation among all EFSs and files.

The proof of Theorem 2 is given in Appendix C.

Remark 2-1: In (18), the term B/V is mainly incurred by balancing the cache hit reward and the storage cost constraints. Intuitively, the larger the value of V , the more focus CPHBL puts on maximizing cache hit rewards, and hence a smaller regret. Nonetheless, this also comes with an increase in the total size of virtual queue backlogs, which is unfavorable for keeping storage costs under the budget. In contrast, the smaller the value of V , the more sensitive CPHBL would be to the increase in the storage costs. As a result, each EFS would constantly update its cached file set with files of different storage costs, leading to inferior cache hit rewards. In practice, the selection of the value of V depends on the design tradeoff of real systems.

Remark 2-2: The last two terms of the regret bound are in the order of $O(1/T + \sqrt{(\log T)/(T + H_{\min})})$. These two

terms are mainly incurred by the online learning procedure with offline historical information and collected online feedback. In the following, we first consider the impact of H_{\min} on the regret bound under a fixed value of time horizon length T . Note that when $H_{\min} = 0$, our problem degenerates to the special case without offline historical information, as considered in our previous work [37]. In this case, the whole regret bound is in the order of $O(1/V + \sqrt{(\log T)/T})$. When the offline historical information is available (*i.e.*, $H_{\min} > 0$), the regret bound would be even lower. Specifically, we consider the following four cases under a fixed value of T .¹

- 1) The first case is when $H_{\min} = O(1)$, *i.e.*, a constant value unrelated to T . Compared to the scenario without offline historical information, though the value of regret bound reduces in this case, its order remains to be $O(1/V + \sqrt{(\log T)/T})$.
- 2) The second case is when $H_{\min} = \Theta(T)$, *i.e.*, the number of offline historical observations is comparable to the length of time horizon. In this case, the regret bound is still in the order of $O(1/V + \sqrt{(\log T)/T})$.
- 3) The third case is when $H_{\min} = \Theta(T \log T)$. In this case, under a sufficiently great length of time horizon T , the regret bound approaches $O(1/V + \sqrt{1/T})$.
- 4) The fourth case is when $H_{\min} = \Omega(T^2 \log T)$, *i.e.*, there is adequate offline historical information. In this case, each EFS proactively leverages offline historical information to acquire highly accurate estimations on file popularities. As a result, the last term in the regret bound becomes even smaller, and the second term becomes dominant. Therefore, the order of the regret decreases to $O(1/V + 1/T)$.

When it comes to the impact of time horizon length T , the regret bound decreases and approaches B/V as the value of T increases. In summary, given a longer time horizon length and more historical information (*i.e.*, larger values of T and H_{\min}), CPHBL achieves a better regret performance. Such results are also verified by numerical simulation in Section VII-C.

VI. DRL BASED BENCHMARK DESIGN

In recent years, deep reinforcement learning (DRL) has been widely adopted in various fields to conduct goal-directed learning and sequential decision making [39] [40]. It deals with agents that learn to make better sequential decisions by interacting with the environment without complicated modeling and too much domain knowledge requirement. In this section, to compare our scheme CPHBL with DRL based approaches, we propose a novel Cache Placement scheme with DRL called *CPDRL* as a baseline for evaluation.

A. Overall Design of CPDRL

Under CPDRL, we view each EFS $n \in \mathcal{N}$ as a DRL agent n which interacts with the environment over time slots. As a result, the original problem turns into a multi-agent DRL problem with N agents. Note that under our settings, such

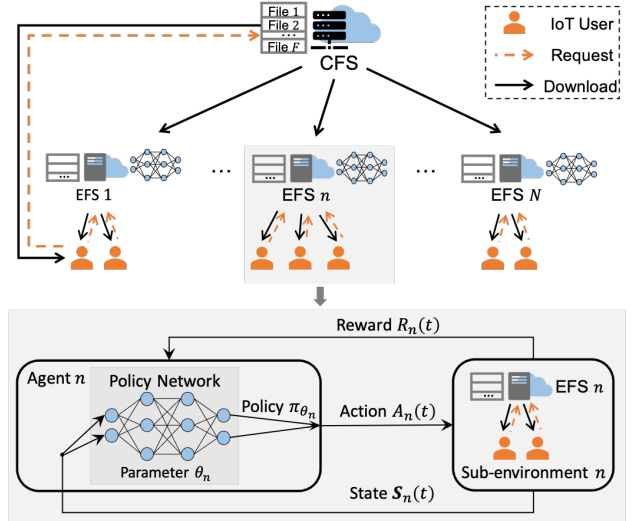


Fig. 4. Overview of CPDRL design. The environment is partitioned into N independent sub-environments, each for an agent (EFS). Note that we do not show the CFS in the sub-environment block. However, in each time slot, each EFS may interact with the CFS for file downloading. In our model, the CFS is assumed to provide simultaneous and independent file deliveries to all EFSs.

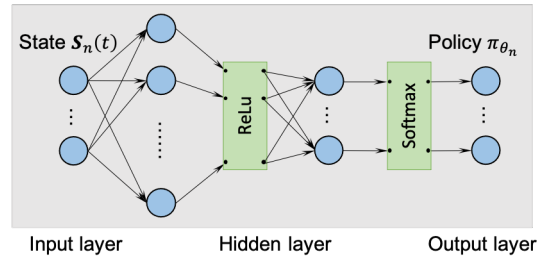


Fig. 5. Design of the policy network for agent n . The cache placement scheme of agent n is designed as a feedforward neural network (FNN) with one hidden layer of dimension 512, followed by a ReLU activation function.

an N -agent DRL problem can be decomposed into N single-agent DRL subproblems since there is no coupling among the agents' decision makings. The reasons are shown as follows. First, the CFS provide simultaneous and independent file deliveries to all EFSs. Second, recall that each IoT user is served by one and only one EFS and thus the subsets of IoT users that are associated with EFSs are disjoint. Based on the above two properties, the decision making on each EFS has no impact on the decisions on other EFSs. Therefore, the environment can be partitioned into N independent sub-environments and each agent n only interacts with its related sub-environment n . As a result, under CPDRL, each agent (EFS) solves for a single-agent DRL subproblem independently. Next, we introduce the basic settings of the single-agent DRL system.

In a classical single-agent DRL system, there is an agent which interacts with its environment over iterations. At the beginning of each iteration t , the agent observes some representation of the environment's state $S(t)$. In response, the agent takes an action $A(t)$ based on its maintained policy π_θ . The policy π_θ is parameterized by a deep neural network

¹The notations O , Θ , and Ω are all asymptotic notations introduced in [38].

(DNN) with parameter θ . After the agent performs the action $A(t)$, it observes a new state $S(t+1)$ and receives a reward $R(t)$. Based on the gained information, the agent improves its policy π_θ to maximize the time-averaged expected reward it receives, i.e., $\mathbb{E}[\frac{1}{T} \sum_{t=0}^{T-1} \gamma^t R(t)]$. Here $\gamma \in [0, 1]$ is called the discount rate and it determines the present value of future rewards.

B. Detailed Design of CPDRL

Considering the limitation of existing DRL techniques, when solving for the cache placement problem (6), we ignore the storage cost constraints (5) in the design of CPDRL. In this subsection, we show our detailed design of CPDRL in terms of the state representation, agent action, and reward signal for a particular agent n .²

1) *State Representation*: We define the observed environment state by agent n in time slot t as $\mathcal{S}_n(t) \triangleq \mathbf{X}_n(t-1)$, i.e., the cache placement on the EFS n in the previous time slot ($t-1$).

2) *Agent Action*: We define the action of agent n in time slot t as a tuple $A_n(t) \in \mathcal{A} \triangleq \{(f, x) | f \in \mathcal{F}, x \in \{0, 1\}\}$. Action $A_n(t) = (f, x)$ means that the agent n updates the cache placement decision for file f on EFS n in time slot t to x . When $x = 1$, file f will be cached on EFS n ; otherwise, file f will not be cached on EFS n .

3) *Reward Design*: The reward received by agent n in time slot t is set as the cache hit reward $R_n(t)$ defined in (4) of Section III-F.

4) *Policy Network*: We design each agent n 's cache placement scheme as a feedforward neural network (FNN) [41] with one hidden layer of dimension 512, followed by a ReLU activation function. We show such a network design in Figure 5. As shown in the figure, the policy network takes the observed environment state as input. When given input $\mathcal{S}_n(t)$, a probability distribution $\pi_{\theta_n}(\cdot | \mathcal{S}_n(t))$ over the action space \mathcal{A} will be output from the network. Note that such a policy network design requires the number of files F to be fixed. The change in the value of F would require the reconstruction and retraining of the policy network. In each time slot, a candidate action will be sampled from set \mathcal{A} according to the distribution $\pi_{\theta_n}(\cdot | \mathcal{S}_n(t))$. The cache placement will be updated accordingly if the sampled action satisfies the storage capacity constraint in (1); otherwise, the cache placement on EFS n will remain unchanged.

C. CPDRL Workflow

We show the pseudocode of CPDRL in Algorithm 2. The operation of CPDRL is composed of two procedures: the cache placement procedure and the policy update procedure. In the *cache placement* procedure, under CPDRL, each EFS makes cache placement decisions based on its current policy network. In the *policy update* procedure, each EFS adopts the policy gradient [42] method to train its policy network with

²In this work, for simplicity, we assume that all of the N agents share the same DRL design, including the same policy network structure and training parameters. In practice, one can employ heterogeneous DRL designs for different agents to adapt to more general scenarios.

Algorithm 2 Cache Placement with Deep Reinforcement Learning (CPDRL)

```

1: Initialize  $\mathbf{X}_n(-1) = \mathbf{0}$  and the policy network  $\pi_{\theta_n}$  for each
   EFS  $n \in \mathcal{N}$ .
2: for each time slot  $t \in \{0, 1, \dots, T-1\}$  do
3:   for each EFS  $n \in \mathcal{N}$  do
4:     %Cache Placement
5:     Observe state  $\mathcal{S}_n(t) \leftarrow \mathbf{X}_n(t-1)$ .
6:     Sample a candidate action  $(f, X'_{n,f}(t))$  from  $\mathcal{A}$  according
7:     to  $\pi_{\theta_n}(\cdot | \mathcal{S}_n(t))$ .
8:     Set  $\mathbf{x}'_n \leftarrow (X_{n,1}(t-1), \dots, X'_{n,f}(t), \dots, X_{n,F}(t-1))$ .
9:     if  $\mathbf{x}'_n$  satisfies the constraint (1) then
10:      Set  $A_n(t) \leftarrow (f, X_{n,f}(t-1))$ .
11:     else
12:      Set  $A_n(t) \leftarrow (f, X'_{n,f}(t))$ .
13:     end if
14:     Perform action  $A_n(t)$  and then receive a reward of  $R_n(t)$ .
15:     %Policy Update
16:     if  $1 \leq t \leq T_0$  and  $t \% l = 0$  then
17:       Train policy network  $\pi_{\theta_n}$  using the collected infor-
18:       mation from time slots  $(t-l+1)$  to  $t$ .
19:     end if
20:   end for
21: end for

```

the collected online feedback. Note that each of the networks is trained during the first T_0 time slots on a batch basis, and the length of each batch is set uniformly as l .

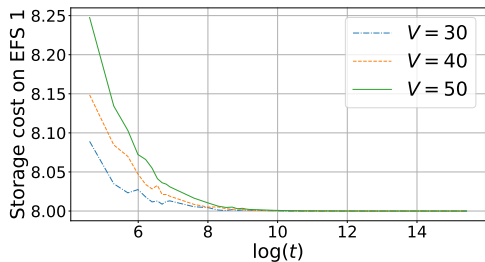
D. Comparison with CPHBL

In comparison with CPHBL, CPDRL has the following limitations. First, it requires the heuristic techniques of network-training or hyper-parameter tuning. Second, its effectiveness can only be justified by experimental simulations without theoretical performance guarantee. Third, it cannot deal with the stochastic time-averaged storage cost constraints. Lastly, it provides few insightful explanations for the resulting decision makings and system performances. In comparison, by employing MAB methods, CPHBL enjoys the advantages of a more lightweight implementation, theoretical tractability, and the applicability to time-averaged constraints. Besides, the design of CPHBL also leads to insightful explanations for the online decision making in previous sections (see remarks in Sections IV–V). We further compare the performance of CPHBL and CPDRL with numerical simulations in Section VII-B.

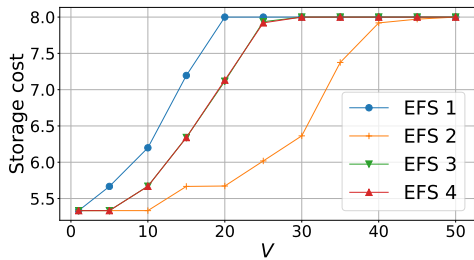
VII. NUMERICAL RESULTS

A. Simulation Settings

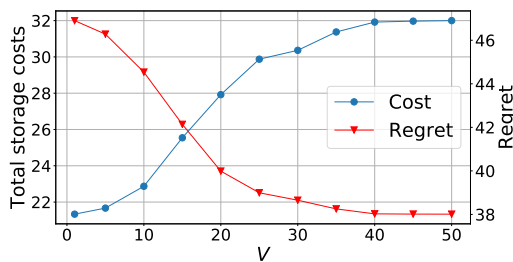
We consider a Fog-assisted IoT system with 1 CFS, 4 EFSs ($N = 4$) and 20 IoT users ($K = 20$). Each user is uniformly randomly assigned to one of the EFSs. The file set \mathcal{F} on the CFS consists of 20 files ($F = 20$) with different file sizes $L_f \in \{1, 2, 4, 8\}$. The storage capacity of each EFS is $M_n = 16$ units. We set the unit storage cost as $\alpha = 1$. We assume that each user k 's requests are generated from a Zipf distribution with a skewness parameter $\gamma \in [0.56, 1.2]$. Note that such skewness parameters are fixed but *unknown* to the EFSs. We set the storage cost budget b_n to be 8 units for each EFS $n \in \mathcal{N}$.



(a) Time-averaged storage cost on EFS 1.



(b) Storage costs on each EFS.



(c) Regret & total storage costs.

Fig. 6. Performance of CPHBL with different values of V .

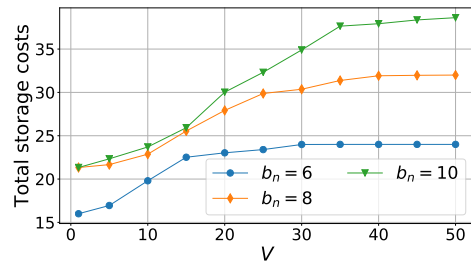
B. Performance of CPHBL with A Fixed Time Horizon Length and A Fixed Number of Offline Historical Observations

In this subsection, we investigate the performance of CPHBL by fixing the time horizon length T as 5×10^6 time slots and the number of offline historical observations $H_{n,f}$ as 1000 for all $n \in \mathcal{N}$, $f \in \mathcal{F}$ (i.e., $H_{\min} = 1000$).

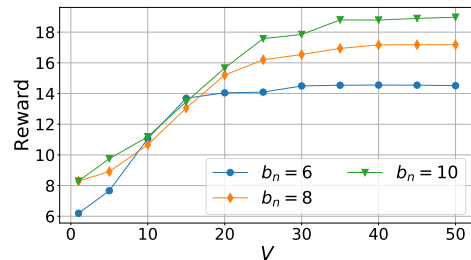
Performance of CPHBL under Different Values of V :

In Figure 6(a), we take the first EFS (EFS 1) as an example to illustrate how the time-averaged storage cost on each EFS changes over time under different values of V . Particularly, on EFS 1, the time-averaged storage cost approaches the cost budget $b_1 = 8$ units as time goes by. Moreover, the greater the value of V , the longer the convergence time. For example, the convergence time extends from 4000 time slots to about 10000 time slots as the value of V increases from 30 to 50. This shows that the larger values of V lead to a longer time for convergence. Figure 6(b) evaluates the time-averaged storage cost on each EFS incurred by CPHBL under different values of V . As the value of parameter V increases, the storage cost on each EFS keeps increasing until it reaches the budget $b_n = 8$ units. Such results show that the time-averaged storage cost constraints in (5) are strictly satisfied under CPHBL.

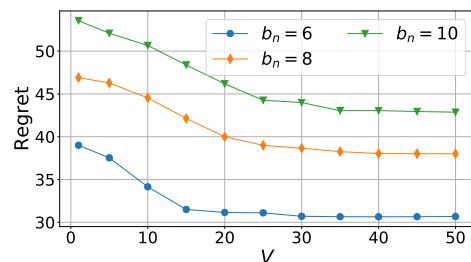
Next, we switch to the evaluations of regrets and total



(a) Time-averaged total storage costs.



(b) Time-averaged total cache hit reward.



(c) Regret.

Fig. 7. Performance of CPHBL given different storage budgets (b_n).

storage costs incurred by CPHBL with different values of V . As shown in Figure 6(c), there is a notable reduction in the regret as the value of V increases. Such results imply that CPHBL can achieve a lower regret with a larger value of V . Moreover, when the value of V is sufficiently large ($V \geq 40$), the regret value stabilizes at around 38.01. This verifies our previous analysis in Theorem 2 about the term B/V in the regret bound (18). Besides, as the value of V increases, we also see an increase in the total storage costs which eventually reach the budget when $V \geq 40$. Overall, the results in Figures 6(b) and 6(c) verify the tunable tradeoff between the regret value and total storage costs.

Performance of CPHBL under Different Settings of Storage Cost Budget b_n : Next, we select different values for the storage cost budget b_n of each EFS n to investigate their impacts on system performances. Figure 7 shows our simulation results. From Figure 7(a), we see that given $V = 50$, the time-averaged total storage costs increase by 60.93% as the value of b_n increases from 6 to 10. Under the same settings, Figure 7(b) shows that the time-averaged total cache hit reward increases by 30.71%. The reason is that with more budget, each EFS would store more files to further maximize the cache hit rewards. Figure 7(c) illustrates the regret under different

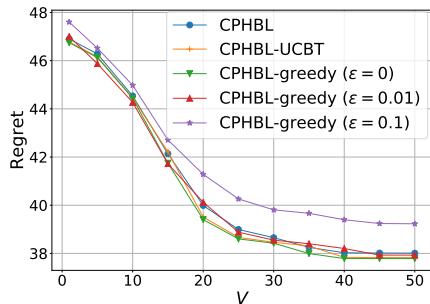


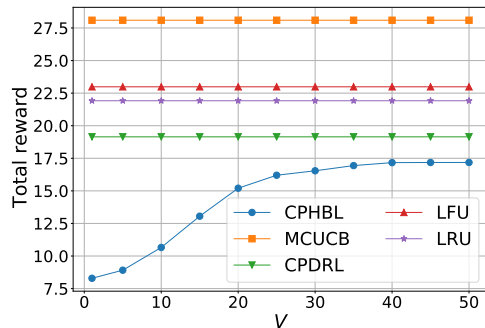
Fig. 8. Regret of CPHBL and its variants.

storage cost budgets. The results verify our theoretical analysis in (17) about the proportional growth of regret with respect to the storage cost budget. The reason is that under CPHBL, each EFS would explore more files when given more budget, thereby resulting in a higher regret.

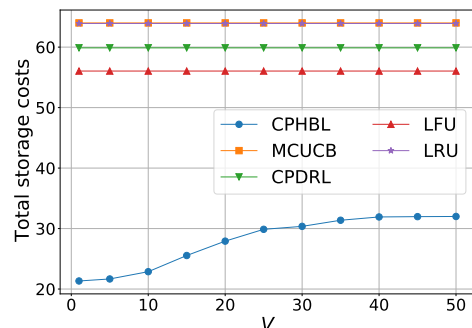
CPHBL vs. Its Variants: In Section IV-B, the confidence radius in (10) measures the uncertainty about the empirical reward estimate. The larger the confidence radius, the greater the necessity of exploration for the corresponding file. Accordingly, each EFS is more prone to caching under-explored files. To investigate how the regret changes under different exploration strategies, we propose two types of variants for CPHBL: one leveraging ε -greedy method and the other employing UCB-like methods. More detail is specified as follows.

- ◇ *CPHBL-greedy*: CPHBL-greedy differs from CPHBL in the cache placement phase (lines 7-9 in Algorithm 1). Specifically, it replaces the HUCB1 estimates $\{\bar{d}_{n,f}(t)\}_{n,f}$ with empirical means $\{\bar{d}_{n,f}(t)\}_{n,f}$ in function SETCACHEPLACEMENT. Recall that $\bar{d}_{n,f}(t)$ denotes the empirical mean that involves both offline historical observations and online feedbacks. Then it adopts ε -greedy method within the cache placement phase. With probability ε , each EFS n selects files uniformly randomly from subset $\mathcal{F}_{n,1}(t)$ to cache. With probability $1 - \varepsilon$, files with the empirically highest reward estimates are chosen to be cached. Intuitively, CPHBL-greedy spends about a proportion ε of time for uniform exploration and the rest $(1 - \varepsilon)$ proportion of time for exploitation.
- ◇ *CPHBL-UCBT*: CPHBL-UCBT replaces the HUCB1 estimate (line 4 in Algorithm 1) with *UCB1-tuned (UCBT)* estimate [43] while the rest remains the same as CPHBL.

We compare the regret value of CPHBL against CPHBL-greedy ($\varepsilon \in \{0, 0.01, 0.1\}$) and CPHBL-UCBT in Figure 8 under different values of V . Regarding the variants of CPHBL, interestingly, although CPHBL-greedy with $\varepsilon = 0$ intuitively discards the chance of uniform exploration in the online learning phase, it still achieves a regret performance that is close to CPHBL, CPHBL-UCBT, and CPHBL-greedy with $\varepsilon = 0.01$. The reason is that CPHBL-greedy with $\varepsilon = 0$ can resort to the storage cost constraint guarantee in the online control phase to conduct enforced exploration. In comparison, the regret of CPHBL-greedy with $\varepsilon = 0.1$ still performs inferior to other schemes due to its over-exploration.



(a) Time-averaged total cache hit reward.



(b) Time-averaged total storage costs.

Fig. 9. Comparison of CPHBL and baseline schemes.

CPHBL vs. Other Baseline Schemes: We also compare the performances of CPHBL with four baseline schemes: MCUCB [33], CPDRL (*Cache Placement with Deep Reinforcement Learning*), LFU (*Least Frequently Used*) [44], and LRU (*Least Recently Used*) [44]. Below we demonstrate how each of them proceeds in detail, respectively.

- ◇ *MCUCB*: Under MCUCB [14], a modified combinatorial UCB scheme is used to estimate file popularities and decide cache placement during each time slot.
- ◇ *CPDRL*: The detailed design of CPDRL is presented in Section VI. In the simulation, we set the network training parameter as $T_0 = 10^6$ and $l = 10$. The policy network parameters are updated using the RMSprop [45] algorithm with a learning rate of 10^{-5} .
- ◇ *LFU*: Under LFU, each EFS maintains a counter for each of its cached files. Each counter records the number of times that its corresponding file has been requested on the EFS. If a requested file is not in the cache, the requested file would be downloaded from the CFS and cached on the EFS by replacing the least frequently used files therein.
- ◇ *LRU*: Under LRU, each EFS records the most recently requested time slot for each of its cached files. If a requested file is not in the cache, the requested file would be downloaded from the CFS and cached on the EFS by replacing the least recently used files.

We show the simulation results in Figure 9. The cache hit rewards and total storage costs of the four baseline schemes

(MCUCB, CPDRL, LFU, and LRU) remain constant given different values of V . This is because their decision making does not involve parameter V . From Figure 9, we see that CPHBL achieves the lowest cache hit reward while MCUCB achieves the highest cache hit reward. Particularly, given $V = 50$, compared to MCUCB, CPHBL achieves a 38.85% lower total cache hit reward. In comparison with the other three baseline schemes, the DRL based scheme CPDRL achieves the worst performance in terms of the cache hit reward. The reason is that it can not learn efficiently from limited online feedback information.

However, except CPHBL, the other four schemes fail to ensure the storage cost constraints in (5).³ More specifically, given $V = 50$, when compared to the four baseline schemes (MCUCB, CPDRL, LFU, and LRU), CPHBL achieves 50.00%, 46.56%, 42.90% and 49.93% reductions in the total storage costs, respectively. Note that such results verify the advantage of our scheme over DRL based approaches.

C. Performance of CPHBL with Different Values of Time Horizon Length and Numbers of Offline Historical Observations

In this subsection, we investigate the impacts of time horizon length T and the number H_{\min} of offline historical observations⁴ on the regret of CPHBL. We take the case when $V = 50$ as an example for illustration. The results are shown in Figure 10.

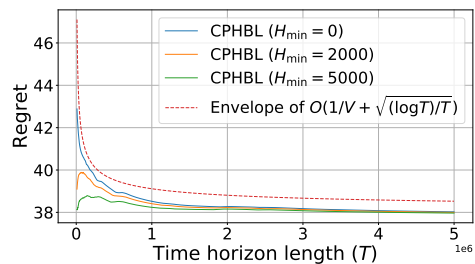
In Figure 10(a), we present the regret performances over a constant time horizon length T under fixed values of H_{\min} . Specifically, each curve corresponds to the result under a constant value of $H_{\min} \in \{0, 2000, 5000\}$ (independent of T). Note that when $H_{\min} = 0$, there is no offline historical information. On one hand, given a fixed number H_{\min} of offline historical observations, the results show that the regret value is reduced by an order of $O(1/V + \sqrt{(\log T)/T})$.⁵ On the other hand, given a fixed value of T , CPHBL achieves a lower regret with more offline historical observations. However, as the value of T becomes sufficiently large, the regret reduction turns negligible. For example, as the value of H_{\min} increases from 0 to 5000, the regret reduces by 0.74% when $T = 10^6$, but only by 0.15% when $T = 5 \times 10^6$.

In Figure 10(b), we compare the regret performances under different values of H_{\min} over various time horizon lengths. Specifically, we consider the cases when $H_{\min} \in \{0, 0.1T, T, T \log T\}$. As shown in the figure, when the value of H_{\min} is small (e.g., when $H_{\min} \leq 0.1T$), even a slight increase in the offline historical information brings a noticeable improvement to the regret performance. However, as the value of H_{\min} increases, the degree of regret reduction

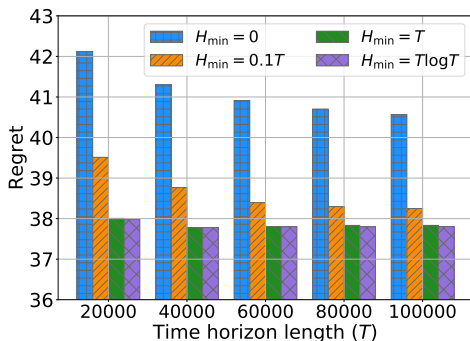
³Recall that the storage cost budget on each EFS is set as $b_n = 8$ units in our simulations. Accordingly, the total time-averaged storage costs of the four EFSs should not exceed 32 units. However, the total time-averaged storage costs all exceed 55 units under the four baseline schemes.

⁴In our simulations, the number $H_{n,f}$ of offline historical observations on EFS n for file f is set to be identical for all $n \in \mathcal{N}$ and $f \in \mathcal{F}$. Therefore, by the definition that $H_{\min} \triangleq \min_{n,f} H_{n,f}$, we have $H_{n,f} = H_{\min}$ for all $n \in \mathcal{N}$ and $f \in \mathcal{F}$.

⁵In Figure 10(a), we provide a curve of $38 + 300\sqrt{(\log T)/T}$ as an envelope of $O(1/V + \sqrt{(\log T)/T})$ for illustration. Note that since V is fixed, $1/V$ can be viewed as a constant term.



(a) Regret with fixed values of H_{\min} when $V = 50$.



(b) Regret with different values of H_{\min} when $V = 50$.

Fig. 10. Regret of CPHBL.

becomes less significant. For example, given $T = 10^5$, the regret reduces by 5.71% as the value of H_{\min} increases from 0 to $0.1T$, but only by 1.09% from $0.1T$ to T . All of the above results verify our theoretical analysis in Theorem 2 (see Section V).

VIII. CONCLUSION

In this paper, we considered the cache placement problem with unknown file popularities in caching-enabled Fog-assisted IoT systems. By formulating the problem as a constrained CMAB problem, we devised a novel proactive cache placement scheme called CPHBL with an effective integration of online control, online learning and offline historical information. Results from our theoretical analysis and numerical simulations showed that our devised scheme achieves a near-optimal total cache hit reward under storage cost constraints with a sublinear time-averaged regret. To the best of our knowledge, our work provided the first systematic study on the synergy of online control, online learning, and offline historical information. Our results not only revealed novel insights to the designers of caching-enabled Fog-assisted IoT systems, but also verified the advantage of CPHBL over the deep reinforcement learning based approach.

REFERENCES

- [1] E. Bastug, M. Bennis, and M. Debbah, "Living on the edge: The role of proactive caching in 5g wireless networks," *IEEE Communications Magazine*, vol. 52, no. 8, pp. 82–89, 2014.
- [2] S. Zhao, Z. Shao, H. Qian, and Y. Yang, "Online user-association with predictive scheduling in wireless caching networks," in *Proceedings of IEEE GLOBECOM*, 2017.

- [3] Y. Jiang, M. Ma, M. Bennis, F. Zheng, and X. You, "A novel caching policy with content popularity prediction and user preference learning in fog-ran," in *Proceedings of IEEE GLOBECOM Workshops*, 2017.
- [4] S. Zhao, Y. Yang, Z. Shao, X. Yang, H. Qian, and C.-X. Wang, "Femos: Fog-enabled multitier operations scheduling in dynamic wireless networks," *IEEE Internet of Things Journal*, vol. 5, no. 2, pp. 1169–1183, 2018.
- [5] X. Gao, X. Huang, S. Bian, Z. Shao, and Y. Yang, "Pora: Predictive offloading and resource allocation in dynamic fog computing systems," *IEEE Internet of Things Journal*, vol. 7, no. 1, pp. 72–87, 2020.
- [6] B. Bharath, K. G. Nagananda, and H. V. Poor, "A learning-based approach to caching in heterogenous small cell networks," *IEEE Transactions on Communications*, vol. 64, no. 4, pp. 1674–1686, 2016.
- [7] H. Pang, L. Gao, and L. Sun, "Joint optimization of data sponsoring and edge caching for mobile video delivery," in *Proceedings of IEEE GLOBECOM*, 2016.
- [8] F. Li, J. Liu, and B. Ji, "Combinatorial sleeping bandits with fairness constraints," in *Proceedings of IEEE INFOCOM*, 2019.
- [9] P. Shivaswamy and T. Joachims, "Multi-armed bandit problems with history," in *Proceedings of AISTATS*, 2012.
- [10] M. J. Neely, "Stochastic network optimization with application to communication and queueing systems," *Synthesis Lectures on Communication Networks*, vol. 3, no. 1, pp. 1–211, 2010.
- [11] J. Kwak, Y. Kim, L. B. Le, and S. Chong, "Hybrid content caching in 5g wireless networks: Cloud versus edge caching," *IEEE Transactions on Wireless Communications*, vol. 17, no. 5, pp. 3030–3045, 2018.
- [12] Y. Wang, W. Wang, Y. Cui, K. G. Shin, and Z. Zhang, "Distributed packet forwarding and caching based on stochastic network utility maximization," *IEEE/ACM Transactions on Networking*, vol. 26, no. 3, pp. 1264–1277, 2018.
- [13] J. Xu, L. Chen, and P. Zhou, "Joint service caching and task offloading for mobile edge computing in dense networks," in *Proceedings of IEEE INFOCOM*, 2018.
- [14] P. Blasco and D. Gündüz, "Learning-based optimization of cache content in a small cell base station," in *Proceedings of IEEE ICC*, 2014.
- [15] —, "Multi-armed bandit optimization of cache content in wireless infostation networks," in *Proceedings of IEEE ISIT*, 2014.
- [16] S. Müller, O. Atan, M. van der Schaar, and A. Klein, "Smart caching in wireless small cell networks via contextual multi-armed bandits," in *Proceedings of IEEE ICC*, 2016.
- [17] X. Zhang, G. Zheng, S. Lambotaran, M. R. Nakhai, and K.-K. Wong, "A learning approach to edge caching with dynamic content library in wireless networks," in *Proceedings of IEEE GLOBECOM*, 2019.
- [18] J. Song, M. Sheng, T. Q. Quek, C. Xu, and X. Wang, "Learning-based content caching and sharing for wireless networks," *IEEE Transactions on Communications*, vol. 65, no. 10, pp. 4309–4324, 2017.
- [19] X. Xu, M. Tao, and C. Shen, "Collaborative multi-agent multi-armed bandit learning for small-cell caching," *IEEE Transactions on Wireless Communications*, vol. 19, no. 4, pp. 2570–2585, 2020.
- [20] S. Ajmal, M. B. Muzammil, A. Jamil, S. M. Abbas, U. Iqbal, and P. Touseef, "Survey on cache schemes in heterogeneous networks using 5g internet of things," in *Proceedings of ACM ICFNDS*, 2019.
- [21] L. Li, G. Zhao, and R. S. Blum, "A survey of caching techniques in cellular networks: Research issues and challenges in content placement and delivery strategies," *IEEE Communications Surveys & Tutorials*, vol. 20, no. 3, pp. 1710–1732, 2018.
- [22] H. Pang, J. Liu, X. Fan, and L. Sun, "Toward smart and cooperative edge caching for 5g networks: A deep learning based approach," in *Proceedings of IEEE/ACM IWQoS*, 2018.
- [23] M. Chen, W. Saad, and C. Yin, "Echo-liquid state deep learning for 360° content transmission and caching in wireless vr networks with cellular-connected uavs," *IEEE Transactions on Communications*, vol. 67, no. 9, pp. 6386–6400, 2019.
- [24] A. Ndikumana, N. H. Tran, K. T. Kim, C. S. Hong *et al.*, "Deep learning based caching for self-driving cars in multi-access edge computing," *IEEE Transactions on Intelligent Transportation Systems*, 2020.
- [25] Z. Liu, H. Song, and D. Pan, "Distributed video content caching policy with deep learning approaches for d2d communication," *IEEE Transactions on Vehicular Technology*, 2020.
- [26] E. Baştuğ, M. Bennis, and M. Debbah, "A transfer learning approach for cache-enabled wireless networks," in *Proceedings of IEEE WiOpt*, 2015.
- [27] A. Sengupta, S. Amuru, R. Tandon, R. M. Buehrer, and T. C. Clancy, "Learning distributed caching strategies in small cell networks," in *Proceedings of ISWCS*, 2014.
- [28] A. Sadeghi, F. Sheikholeslami, A. G. Marques, and G. B. Giannakis, "Reinforcement learning for adaptive caching with dynamic storage pricing," *IEEE Journal on Selected Areas in Communications*, vol. 37, no. 10, pp. 2267–2281, 2019.
- [29] Z. Zhu, T. Liu, S. Jin, and X. Luo, "Learn and pick right nodes to offload," in *Proceedings of IEEE GLOBECOM*, 2018.
- [30] J. Yao and N. Ansari, "Energy-aware task allocation for mobile iot by online reinforcement learning," in *Proceedings of IEEE ICC*, 2019.
- [31] A. Mukherjee, S. Misra, V. S. P. Chandra, and M. S. Obaidat, "Resource-optimized multiarmed bandit-based offload path selection in edge uav swarms," *IEEE Internet of Things Journal*, vol. 6, no. 3, pp. 4889–4896, 2018.
- [32] D. López-Pérez, A. Valcarce, G. De La Roche, and J. Zhang, "Ofdma femtocells: A roadmap on interference avoidance," *IEEE Communications Magazine*, vol. 47, no. 9, pp. 41–48, 2009.
- [33] W. Chen, Y. Wang, and Y. Yuan, "Combinatorial multi-armed bandit: General framework and applications," in *Proceedings of ICML*, 2013.
- [34] A. Slivkins *et al.*, "Introduction to multi-armed bandits," *Foundations and Trends® in Machine Learning*, vol. 12, no. 1-2, pp. 1–286, 2019.
- [35] S. Martello, D. Pisinger, and P. Toth, "Dynamic programming and strong bounds for the 0-1 knapsack problem," *Management Science*, vol. 45, no. 3, pp. 414–424, 1999.
- [36] —, "New trends in exact algorithms for the 0–1 knapsack problem," *European Journal of Operational Research*, vol. 123, no. 2, pp. 325–332, 2000.
- [37] X. Gao, X. Huang, Y. Tang, Z. Shao, and Y. Yang, "Proactive cache placement with bandit learning in fog-assisted iot system," in *Proceedings of IEEE ICC*, 2020.
- [38] T. H. Cormen, C. E. Leiserson, R. L. Rivest, and C. Stein, *Introduction to Algorithms*. MIT press, 2009.
- [39] S. Bian, X. Huang, Z. Shao, and Y. Yang, "Neural task scheduling with reinforcement learning for fog computing systems," in *Proceedings of IEEE GLOBECOM*, 2019.
- [40] J. Pei, P. Hong, M. Pan, J. Liu, and J. Zhou, "Optimal vnf placement via deep reinforcement learning in sdn/nfv-enabled networks," *IEEE Journal on Selected Areas in Communications*, vol. 38, no. 2, pp. 263–278, 2019.
- [41] B. Irie and S. Miyake, "Capabilities of three-layered perceptrons," in *Proceedings of ICNN*, 1988.
- [42] R. S. Sutton, D. A. McAllester, S. P. Singh, and Y. Mansour, "Policy gradient methods for reinforcement learning with function approximation," in *Proceedings of NeurIPS*, 2000.
- [43] P. Auer, N. Cesa-Bianchi, and P. Fischer, "Finite-time analysis of the multiarmed bandit problem," *Machine Learning*, vol. 47, no. 2-3, pp. 235–256, 2002.
- [44] D. Lee, J. Choi, J.-H. Kim, S. H. Noh, S. L. Min, Y. Cho, and C. S. Kim, "Lrfu: A spectrum of policies that subsumes the least recently used and least frequently used policies," *IEEE Transactions on Computers*, vol. 50, no. 12, pp. 1352–1361, 2001.
- [45] G. Hinton, N. Srivastava, and K. Swersky, "Overview of mini-batch gradient descent," *Neural Networks for Machine Learning*, vol. 575, no. 8, 2012.
- [46] W. Hoeffding, "Probability inequalities for sums of bounded random variables," in *The Collected Works of Wassily Hoeffding*. Springer, 1994, pp. 409–426.

APPENDIX A ALGORITHM DEVELOPMENT

We define a Lyapunov function as follows:

$$L(\mathbf{Q}(t)) \triangleq \frac{1}{2} \sum_{n \in \mathcal{N}} (Q_n(t))^2, \quad (19)$$

in which $\mathbf{Q}(t) = (Q_1(t), Q_2(t), \dots, Q_N(t))$ is the vector of all virtual queues. Then we have

$$\begin{aligned} & L(\mathbf{Q}(t+1)) - L(\mathbf{Q}(t)) \\ &= \frac{1}{2} \sum_{n \in \mathcal{N}} \left[(Q_n(t+1))^2 - (Q_n(t))^2 \right] \\ &\leq \frac{1}{2} \sum_{n \in \mathcal{N}} \left[b_n^2 + (C_n(t))^2 + 2Q_n(t)(C_n(t) - b_n) \right]. \end{aligned} \quad (20)$$

Since $C_n(t) = \sum_{f \in \mathcal{F}} \alpha L_f X_{n,f}(t) \leq \alpha M_n$, it follows that

$$L(\mathbf{Q}(t+1)) - L(\mathbf{Q}(t)) \leq B + \sum_{n \in \mathcal{N}} Q_n(t) (C_n(t) - b_n), \quad (21)$$

where $B \triangleq \frac{1}{2} \sum_{n \in \mathcal{N}} (b_n^2 + \alpha^2 M_n^2)$.

We consider an optimal cache placement scheme which makes *i.i.d.* cache placement decisions $\mathbf{X}^*(t)$ in each time slot t , then the optimal time-averaged expected total reward of all EFSs is

$$R^* = \frac{1}{T} \sum_{t=0}^{T-1} \sum_{n \in \mathcal{N}} \mathbb{E} \left[\hat{R}_n(\mathbf{X}_n^*(t)) \right]. \quad (22)$$

According to (7), the regret of cache placement scheme $\{\mathbf{X}(t)\}_t$ over T time slots is

$$Reg(T) = \frac{1}{T} \sum_{t=0}^{T-1} \sum_{n \in \mathcal{N}} \mathbb{E} \left[\hat{R}_n(\mathbf{X}_n^*(t)) - \hat{R}_n(\mathbf{X}_n(t)) \right]. \quad (23)$$

By the definition of reward $\hat{R}_n(\cdot)$ in (4), it follows that

$$Reg(T) = \frac{1}{T} \sum_{t=0}^{T-1} \sum_{n \in \mathcal{N}} \sum_{f \in \mathcal{F}} L_f \left(\mathbb{E} [D_{n,f}(t) X_{n,f}^*(t)] - \mathbb{E} [D_{n,f}(t) X_{n,f}(t)] \right). \quad (24)$$

Since the cache placement decision $X_{n,f}(t)$ is determined when $D_{n,f}(t)$ is unknown, $X_{n,f}(t)$ is independent of the $D_{n,f}(t)$. On the other hand, $X_{n,f}^*(t)$ is *i.i.d.* over time slots and it is also independent of $D_{n,f}(t)$. Then by $\mathbb{E}[D_{n,f}(t)] = d_{n,f}$, we have

$$Reg(T) = \frac{1}{T} \sum_{t=0}^{T-1} \sum_{n \in \mathcal{N}} \sum_{f \in \mathcal{F}} L_f d_{n,f} \mathbb{E} [X_{n,f}^*(t) - X_{n,f}(t)]. \quad (25)$$

We define the one-time-slot regret in each time slot t as

$$\Delta_{Reg}(t) \triangleq \sum_{n \in \mathcal{N}} \sum_{f \in \mathcal{F}} L_f d_{n,f} (X_{n,f}^*(t) - X_{n,f}(t)). \quad (26)$$

The regret $Reg(T)$ can be expressed as

$$Reg(T) = \frac{1}{T} \sum_{t=0}^{T-1} \mathbb{E} [\Delta_{Reg}(t)]. \quad (27)$$

Then we define the Lyapunov drift-plus-regret as

$$\Delta_V(\mathbf{Q}(t)) \triangleq \mathbb{E} [L(\mathbf{Q}(t+1)) - L(\mathbf{Q}(t)) | \mathbf{Q}(t)] + V \mathbb{E} [\Delta_{Reg}(t) | \mathbf{Q}(t)]. \quad (28)$$

By (21) and (26), it follows that

$$\begin{aligned} \Delta_V(\mathbf{Q}(t)) &\leq B + V \mathbb{E} \left[\sum_{n \in \mathcal{N}} \sum_{f \in \mathcal{F}} L_f d_{n,f} X_{n,f}^*(t) | \mathbf{Q}(t) \right] \\ &\quad + \mathbb{E} \left[\sum_{n \in \mathcal{N}} Q_n(t) (C_n(t) - b_n) | \mathbf{Q}(t) \right] \\ &\quad - V \mathbb{E} \left[\sum_{n \in \mathcal{N}} \sum_{f \in \mathcal{F}} L_f d_{n,f} X_{n,f}(t) | \mathbf{Q}(t) \right]. \end{aligned} \quad (29)$$

Since $\tilde{d}_{n,f}(t)$ is the HUCB1 estimate of $d_{n,f}$ in time slot t such that $\tilde{d}_{n,f}(t) \in [0, K_n]$, we have

$$\begin{aligned} &\sum_{n \in \mathcal{N}} \sum_{f \in \mathcal{F}} L_f d_{n,f} X_{n,f}(t) \\ &= \sum_{n \in \mathcal{N}} \sum_{f \in \mathcal{F}} L_f \tilde{d}_{n,f}(t) X_{n,f}(t) \\ &\quad + \sum_{n \in \mathcal{N}} \sum_{f \in \mathcal{F}} L_f (d_{n,f} - \tilde{d}_{n,f}(t)) X_{n,f}(t) \\ &\stackrel{(a)}{\geq} \sum_{n \in \mathcal{N}} \sum_{f \in \mathcal{F}} L_f \tilde{d}_{n,f}(t) X_{n,f}(t) \\ &\quad - \sum_{n \in \mathcal{N}} K_n \sum_{f \in \mathcal{F}} L_f X_{n,f}(t) \\ &\stackrel{(b)}{\geq} \sum_{n \in \mathcal{N}} \sum_{f \in \mathcal{F}} L_f \tilde{d}_{n,f}(t) X_{n,f}(t) - \sum_{n \in \mathcal{N}} K_n M_n, \end{aligned} \quad (30)$$

where inequality (a) holds because that $d_{n,f}, \tilde{d}_{n,f}(t) \in [0, K_n]$ and inequality (b) is due to that $\sum_{f \in \mathcal{F}} L_f X_{n,f}(t) \leq M_n$. Then it follows that

$$\begin{aligned} \Delta_V(\mathbf{Q}(t)) &\leq B + \sum_{n \in \mathcal{N}} V K_n M_n \\ &\quad + V \mathbb{E} \left[\sum_{n \in \mathcal{N}} \sum_{f \in \mathcal{F}} L_f d_{n,f} X_{n,f}^*(t) | \mathbf{Q}(t) \right] \\ &\quad + \mathbb{E} \left[\sum_{n \in \mathcal{N}} Q_n(t) (C_n(t) - b_n) | \mathbf{Q}(t) \right] \\ &\quad - V \mathbb{E} \left[\sum_{n \in \mathcal{N}} \sum_{f \in \mathcal{F}} L_f \tilde{d}_{n,f}(t) X_{n,f}(t) | \mathbf{Q}(t) \right]. \end{aligned} \quad (31)$$

Substituting (2) and (4) into above inequality, we have

$$\begin{aligned} \Delta_V(\mathbf{Q}(t)) &\leq B + \sum_{n \in \mathcal{N}} V K_n M_n - \sum_{n \in \mathcal{N}} Q_n(t) b_n \\ &\quad + V \mathbb{E} \left[\sum_{n \in \mathcal{N}} \sum_{f \in \mathcal{F}} L_f d_{n,f} X_{n,f}^*(t) | \mathbf{Q}(t) \right] \\ &\quad - \mathbb{E} \left[\sum_{n \in \mathcal{N}} \sum_{f \in \mathcal{F}} \tilde{w}_{n,f}(t) X_{n,f}(t) | \mathbf{Q}(t) \right], \end{aligned} \quad (32)$$

where $\tilde{w}_{n,f}(t)$ is defined as

$$\tilde{w}_{n,f}(t) \triangleq L_f \left(V \tilde{d}_{n,f}(t) - \alpha Q_n(t) \right). \quad (33)$$

To minimize the upper bound of drift-plus-regret $\Delta_V(\mathbf{Q}(t))$ in (32), we switch to solving the following problem in each time slot t :

$$\begin{aligned} &\underset{\mathbf{X}(t)}{\text{maximize}} && \sum_{n \in \mathcal{N}} \sum_{f \in \mathcal{F}} \tilde{w}_{n,f}(t) X_{n,f}(t) \\ &\text{subject to} && \sum_{f \in \mathcal{F}} L_f X_{n,f}(t) \leq M_n, \forall n \in \mathcal{N}, \\ &&& X_{n,f}(t) \in \{0, 1\}, \forall n \in \mathcal{N}, f \in \mathcal{F}. \end{aligned} \quad (34)$$

In fact, problem (34) can be further decoupled into N sub-problems. For each EFS $n \in \mathcal{N}$, we solve the following

subproblem for the cache placement vector $\mathbf{X}_n(t)$ in time slot t :

$$\begin{aligned} & \underset{\mathbf{X}_n(t)}{\text{maximize}} && \sum_{f \in \mathcal{F}} \tilde{w}_{n,f}(t) X_{n,f}(t) \\ & \text{subject to} && \sum_{f \in \mathcal{F}} L_f X_{n,f}(t) \leq M_n, \\ & && X_{n,f}(t) \in \{0, 1\}, \forall f \in \mathcal{F}. \end{aligned} \quad (35)$$

■

APPENDIX B PROOF OF THEOREM 1

First, we have the following lemma.

Lemma 1: If the budget vector \mathbf{b} is an interior point of the maximal feasible region \mathcal{B} , then there exists a feasible scheme which makes *i.i.d.* decision over time independent of the virtual queue backlog sizes.

The proof is omitted since it is quite standard as shown in the proof of Lemma 1 in [8].

Then based on Lemma 1, we begin to prove Theorem 1. By our assumption in Theorem 1 that \mathbf{b} is an interior point of \mathcal{B} , there must exist some $\epsilon > 0$ such that $\mathbf{b} - \epsilon \mathbf{1}$ is also an interior point of \mathcal{B} . Here $\mathbf{1}$ denotes the N -dimensional all-ones vector. Then by Lemma 1, since $\mathbf{b} - \epsilon \mathbf{1}$ lies in the interior of \mathcal{B} , there exists a feasible scheme which makes *i.i.d.* decision over time independent of the virtual queue backlog sizes such that

$$\mathbb{E} \left[\hat{C}_n(\mathbf{X}_n^\epsilon(t)) \right] \leq b_n - \epsilon, \quad \forall n \in \mathcal{N}, t, \quad (36)$$

where $\mathbf{X}^\epsilon(t) \triangleq (\mathbf{X}_1^\epsilon(t), \mathbf{X}_2^\epsilon(t), \dots, \mathbf{X}_N^\epsilon(t))$ is the cache placement decision vector during time slot t under the scheme. We denote the cache placement decision vector during time slot t under our scheme CPHBL by $\mathbf{X}^c(t) \triangleq (\mathbf{X}_1^c(t), \mathbf{X}_2^c(t), \dots, \mathbf{X}_N^c(t))$, which is the optimal solution of problem (34). Then based on (31), we have

$$\begin{aligned} \Delta_V(\mathbf{Q}(t)) & \leq B + \sum_{n \in \mathcal{N}} V K_n M_n \\ & + V \mathbb{E} \left[\sum_{n \in \mathcal{N}} \sum_{f \in \mathcal{F}} L_f d_{n,f} X_{n,f}^*(t) \mid \mathbf{Q}(t) \right] \\ & + \mathbb{E} \left[\sum_{n \in \mathcal{N}} Q_n(t) \left(\hat{C}_n(\mathbf{X}_n^c(t)) - b_n \right) \mid \mathbf{Q}(t) \right] \\ & - V \mathbb{E} \left[\sum_{n \in \mathcal{N}} \sum_{f \in \mathcal{F}} L_f \tilde{d}_{n,f}(t) X_{n,f}^c(t) \mid \mathbf{Q}(t) \right] \\ & \leq B + \sum_{n \in \mathcal{N}} V K_n M_n \\ & + V \mathbb{E} \left[\sum_{n \in \mathcal{N}} \sum_{f \in \mathcal{F}} L_f d_{n,f} X_{n,f}^*(t) \mid \mathbf{Q}(t) \right] \\ & + \mathbb{E} \left[\sum_{n \in \mathcal{N}} Q_n(t) \left(\hat{C}_n(\mathbf{X}_n^\epsilon(t)) - b_n \right) \mid \mathbf{Q}(t) \right] \\ & - V \mathbb{E} \left[\sum_{n \in \mathcal{N}} \sum_{f \in \mathcal{F}} L_f \tilde{d}_{n,f}(t) X_{n,f}^\epsilon(t) \mid \mathbf{Q}(t) \right], \end{aligned} \quad (37)$$

where $B \triangleq \frac{1}{2} \sum_{n \in \mathcal{N}} (b_n^2 + \alpha^2 M_n^2)$. Since $\mathbf{X}^\epsilon(t)$ is independent of $\mathbf{Q}(t)$, we have

$$\begin{aligned} \Delta_V(\mathbf{Q}(t)) & \leq B + \sum_{n \in \mathcal{N}} V K_n M_n \\ & + V \mathbb{E} \left[\sum_{n \in \mathcal{N}} \sum_{f \in \mathcal{F}} L_f d_{n,f} X_{n,f}^*(t) \mid \mathbf{Q}(t) \right] \\ & + \sum_{n \in \mathcal{N}} Q_n(t) \mathbb{E} \left[\hat{C}_n(\mathbf{X}_n^\epsilon(t)) - b_n \right] \\ & - V \mathbb{E} \left[\sum_{n \in \mathcal{N}} \sum_{f \in \mathcal{F}} L_f \tilde{d}_{n,f}(t) X_{n,f}^\epsilon(t) \mid \mathbf{Q}(t) \right]. \end{aligned} \quad (38)$$

By (36), it follows that

$$\begin{aligned} \Delta_V(\mathbf{Q}(t)) & \leq B + \sum_{n \in \mathcal{N}} V K_n M_n - \epsilon \sum_{n \in \mathcal{N}} Q_n(t) \\ & + V \mathbb{E} \left[\sum_{n \in \mathcal{N}} \sum_{f \in \mathcal{F}} L_f d_{n,f} X_{n,f}^*(t) \mid \mathbf{Q}(t) \right] \\ & - V \mathbb{E} \left[\sum_{n \in \mathcal{N}} \sum_{f \in \mathcal{F}} L_f \tilde{d}_{n,f}(t) X_{n,f}^\epsilon(t) \mid \mathbf{Q}(t) \right]. \end{aligned} \quad (39)$$

Since $\sum_{f \in \mathcal{F}} L_f d_{n,f} X_{n,f}^*(t) \leq K_n \sum_{f \in \mathcal{F}} L_f X_{n,f}^*(t) \leq K_n b_n$ and $\tilde{d}_{n,f} X_{n,f}^\epsilon(t) \geq 0$, we have

$$\Delta_V(\mathbf{Q}(t)) \leq B + V \sum_{n \in \mathcal{N}} 2K_n M_n - \epsilon \sum_{n \in \mathcal{N}} Q_n(t). \quad (40)$$

Substituting (28) into above inequality, we have

$$\begin{aligned} \mathbb{E} [L(\mathbf{Q}(t+1)) - L(\mathbf{Q}(t)) \mid \mathbf{Q}(t)] + V \mathbb{E} [\Delta_{Reg}(t) \mid \mathbf{Q}(t)] \\ \leq B + V \sum_{n \in \mathcal{N}} 2K_n M_n - \epsilon \sum_{n \in \mathcal{N}} Q_n(t). \end{aligned} \quad (41)$$

Taking expectation at both sides of above inequality and summing it over time slots $\{0, 1, \dots, T'-1\}$, we have

$$\begin{aligned} \mathbb{E} [L(\mathbf{Q}(T'))] - \mathbb{E} [L(\mathbf{Q}(0))] + V \sum_{t=0}^{T'-1} \mathbb{E} [\Delta_{Reg}(t)] \\ \leq T' B + T' V \sum_{n \in \mathcal{N}} 2K_n M_n - \epsilon \sum_{t=0}^{T'-1} \sum_{n \in \mathcal{N}} \mathbb{E} [Q_n(t)]. \end{aligned} \quad (42)$$

Dividing at both sides by $T'\epsilon$ and rearrange the terms, we have

$$\begin{aligned} \frac{1}{T'} \sum_{t=0}^{T'-1} \sum_{n \in \mathcal{N}} \mathbb{E} [Q_n(t)] \leq \frac{1}{\epsilon} \left(B + V \sum_{n \in \mathcal{N}} 2K_n M_n \right) \\ + \frac{\mathbb{E} [L(\mathbf{Q}(0))]}{T'\epsilon} - \frac{\mathbb{E} [L(\mathbf{Q}(T'))]}{T'\epsilon} - \frac{V}{T'\epsilon} \sum_{t=0}^{T'-1} \mathbb{E} [\Delta_{Reg}(t)]. \end{aligned} \quad (43)$$

It follows by the fact $L(\mathbf{Q}(0)) = 0$, $L(\mathbf{Q}(T')) \geq 0$, and $\frac{1}{T'} \sum_{t=0}^{T'-1} \mathbb{E} [\Delta_{Reg}(t)] = Reg(T') \geq 0$ that

$$\frac{1}{T'} \sum_{t=0}^{T'-1} \sum_{n \in \mathcal{N}} \mathbb{E} [Q_n(t)] \leq \frac{B + V \sum_{n \in \mathcal{N}} 2K_n M_n}{\epsilon}. \quad (44)$$

By taking the limsup of the left-hand-side term in above inequality as $T' \rightarrow \infty$, we obtain

$$\limsup_{T' \rightarrow \infty} \frac{1}{T'} \sum_{t=0}^{T'-1} \sum_{n \in \mathcal{N}} \mathbb{E}[Q_n(t)] \leq \frac{B + V \sum_{n \in \mathcal{N}} 2K_n M_n}{\epsilon}. \quad (45)$$

This implies that $\limsup_{T' \rightarrow \infty} \frac{1}{T'} \sum_{t=0}^{T'-1} \mathbb{E}[Q_n(t)] < \infty$ and the virtual queueing process $\{Q_n\}_t$ defined in (13) is strongly stable for each EFS $n \in \mathcal{N}$. Hence, the time-averaged storage cost constraints in (5) are satisfied. ■

APPENDIX C PROOF OF THEOREM 2

By Lemma 1, since \mathbf{b} lies in the interior of \mathcal{B} , there exists an optimal scheme which makes *i.i.d.* decision over time independent of the virtual queue backlog sizes such that

$$\mathbb{E} \left[\hat{C}_n(\mathbf{X}_n^*(t)) \right] \leq b_n, \quad \forall n \in \mathcal{N}, t, \quad (46)$$

where $\mathbf{X}^*(t) \triangleq (\mathbf{X}_1^*(t), \mathbf{X}_2^*(t), \dots, \mathbf{X}_N^*(t))$ is the cache placement decision vector in time slot t under the optimal scheme. By the inequality in (21) and the definition (26), under CPDBL, we have

$$\begin{aligned} & L(\mathbf{Q}(t+1)) - L(\mathbf{Q}(t)) + V\Delta_{Reg}(t) \\ & \leq B + \sum_{n \in \mathcal{N}} Q_n(t) \left(\hat{C}_n(\mathbf{X}_n^c(t)) - b_n \right) \\ & \quad - V \sum_{n \in \mathcal{N}} \sum_{f \in \mathcal{F}} L_f d_{n,f} (X_{n,f}^*(t) - X_{n,f}^c(t)). \end{aligned} \quad (47)$$

The inequality above can be equivalently written as

$$\begin{aligned} & L(\mathbf{Q}(t+1)) - L(\mathbf{Q}(t)) + V\Delta_{Reg}(t) \\ & \leq B + \sum_{n \in \mathcal{N}} Q_n(t) \left(\hat{C}_n(\mathbf{X}_n^*(t)) - b_n \right) \\ & \quad + \sum_{n \in \mathcal{N}} \left(\sum_{f \in \mathcal{F}} V L_f d_{n,f} X_{n,f}^*(t) - Q_n(t) \hat{C}_n(\mathbf{X}_n^*(t)) \right) \\ & \quad - \sum_{n \in \mathcal{N}} \left(\sum_{f \in \mathcal{F}} V L_f d_{n,f} X_{n,f}^c(t) - Q_n(t) \hat{C}_n(\mathbf{X}_n^c(t)) \right). \end{aligned} \quad (48)$$

Substituting (2) into the above inequality, we have

$$\begin{aligned} & L(\mathbf{Q}(t+1)) - L(\mathbf{Q}(t)) + V\Delta_{Reg}(t) \\ & \leq B + \sum_{n \in \mathcal{N}} Q_n(t) \left(\hat{C}_n(\mathbf{X}_n^*(t)) - b_n \right) \\ & \quad + \sum_{n \in \mathcal{N}} \sum_{f \in \mathcal{F}} L_f (V d_{n,f} - \alpha Q_n(t)) X_{n,f}^*(t) \\ & \quad - \sum_{n \in \mathcal{N}} \sum_{f \in \mathcal{F}} L_f (V d_{n,f} - \alpha Q_n(t)) X_{n,f}^c(t). \end{aligned} \quad (49)$$

For each EFS $n \in \mathcal{N}$ and each file $f \in \mathcal{F}$, we define

$$w_{n,f}(t) \triangleq L_f (V d_{n,f} - \alpha Q_n(t)). \quad (50)$$

Then inequality (49) can be simplified as:

$$\begin{aligned} & L(\mathbf{Q}(t+1)) - L(\mathbf{Q}(t)) + V\Delta_{Reg}(t) \\ & \leq B + \sum_{n \in \mathcal{N}} Q_n(t) \left(\hat{C}_n(\mathbf{X}_n^*(t)) - b_n \right) \\ & \quad + \sum_{n \in \mathcal{N}} \sum_{f \in \mathcal{F}} w_{n,f}(t) (X_{n,f}^*(t) - X_{n,f}^c(t)). \end{aligned} \quad (51)$$

For simplicity of expression, we define

$$\Phi_1(t) \triangleq \sum_{n \in \mathcal{N}} \sum_{f \in \mathcal{F}} w_{n,f}(t) (X_{n,f}^*(t) - X_{n,f}^c(t)). \quad (52)$$

It follows that

$$\begin{aligned} & L(\mathbf{Q}(t+1)) - L(\mathbf{Q}(t)) + V\Delta_{Reg}(t) \\ & \leq B + \Phi_1(t) + \sum_{n \in \mathcal{N}} Q_n(t) (\hat{C}_n(\mathbf{X}_n^*(t)) - b_n). \end{aligned} \quad (53)$$

Taking conditional expectation at both sides of above inequality, we have

$$\begin{aligned} & \mathbb{E} [L(\mathbf{Q}(t+1)) - L(\mathbf{Q}(t)) | \mathbf{Q}(t)] + V\mathbb{E} [\Delta_{Reg}(t) | \mathbf{Q}(t)] \\ & \leq B + \mathbb{E} [\Phi_1(t) | \mathbf{Q}(t)] \\ & \quad + \mathbb{E} \left[\sum_{n \in \mathcal{N}} Q_n(t) (\hat{C}_n(\mathbf{X}_n^*(t)) - b_n) | \mathbf{Q}(t) \right] \\ & = B + \mathbb{E} [\Phi_1(t) | \mathbf{Q}(t)] \\ & \quad + \sum_{n \in \mathcal{N}} Q_n(t) \left(\mathbb{E} [\hat{C}_n(\mathbf{X}_n^*(t))] - b_n \right). \end{aligned} \quad (55)$$

The last equality holds because that $\hat{C}_n(\mathbf{X}_n^*(t))$ is independent of $\mathbf{Q}(t)$. By the inequalities in (46), it follows that

$$\begin{aligned} & \mathbb{E} [L(\mathbf{Q}(t+1)) - L(\mathbf{Q}(t)) | \mathbf{Q}(t)] \\ & \quad + V\mathbb{E} [\Delta_{Reg}(t) | \mathbf{Q}(t)] \leq B + \mathbb{E} [\Phi_1(t) | \mathbf{Q}(t)]. \end{aligned} \quad (56)$$

Taking expectation at both sides of above inequality, we have

$$\begin{aligned} & \mathbb{E} [L(\mathbf{Q}(t+1)) - L(\mathbf{Q}(t))] + V\mathbb{E} [\Delta_{Reg}(t)] \\ & \leq B + \mathbb{E} [\Phi_1(t)]. \end{aligned} \quad (57)$$

Summing above inequality over time slots $\{0, 1, \dots, T-1\}$ and dividing it at both sides by TV , we have

$$\begin{aligned} & \frac{\mathbb{E} [L(\mathbf{Q}(T))]}{TV} - \frac{\mathbb{E} [L(\mathbf{Q}(0))]}{TV} + \frac{1}{T} \sum_{t=0}^{T-1} \mathbb{E} [\Delta_{Reg}(t)] \\ & \leq \frac{B}{V} + \frac{1}{TV} \sum_{t=0}^{T-1} \mathbb{E} [\Phi_1(t)]. \end{aligned} \quad (58)$$

Since $L(\mathbf{Q}(0))$ and $L(\mathbf{Q}(T))$ are both non-negative, it follows that

$$\begin{aligned} & Reg(T) = \frac{1}{T} \sum_{t=0}^{T-1} \mathbb{E} [\Delta_{Reg}(t)] \\ & \leq \frac{B}{V} + \frac{1}{TV} \sum_{t=0}^{T-1} \mathbb{E} [\Phi_1(t)]. \end{aligned} \quad (59)$$

Next, we bound $\Phi_1(t)$ to obtain the upper bound of the regret $Reg(T)$.

A. Bounding $\Phi_1(t)$

To find the upper bound of $\Phi_1(t)$. Consider a cache placement scheme which makes a placement decision during each time slot t , denoted by vector $\mathbf{X}'(t) \triangleq$

$(\mathbf{X}'_1(t), \mathbf{X}'_2(t), \dots, \mathbf{X}'_N(t))$ with each entry $\mathbf{X}'_n(t)$ as the optimal solution of the following problem:

$$\begin{aligned} & \underset{\mathbf{X}_n(t)}{\text{maximize}} && \sum_{f \in \mathcal{F}} w_{n,f}(t) X_{n,f}(t) \\ & \text{subject to} && \sum_{f \in \mathcal{F}} L_f X_{n,f}(t) \leq M_n, \\ & && X_{n,f}(t) \in \{0, 1\}, \forall f \in \mathcal{F}. \end{aligned} \quad (60)$$

Since $\mathbf{X}_n^*(t)$ is a feasible solution of problem (60), we have

$$\sum_{f \in \mathcal{F}} w_{n,f}(t) X'_{n,f}(t) \geq \sum_{f \in \mathcal{F}} w_{n,f}(t) X_{n,f}^*(t). \quad (61)$$

It follows that

$$\begin{aligned} \Phi_1(t) &= \sum_{n \in \mathcal{N}} \sum_{f \in \mathcal{F}} w_{n,f}(t) (X_{n,f}^*(t) - X_{n,f}^c(t)) \\ &\leq \sum_{n \in \mathcal{N}} \sum_{f \in \mathcal{F}} w_{n,f}(t) (X'_{n,f}(t) - X_{n,f}^c(t)) \\ &\leq \sum_{n \in \mathcal{N}} \sum_{f \in \mathcal{F}} w_{n,f}(t) (X'_{n,f}(t) - X_{n,f}^c(t)) \\ &\quad + \sum_{n \in \mathcal{N}} \sum_{f \in \mathcal{F}} \tilde{w}_{n,f}(t) (X_{n,f}^c(t) - X'_{n,f}(t)). \end{aligned} \quad (62)$$

The last inequality holds since $\mathbf{X}_n^c(t)$ is the optimal solution of problem (14) but $\mathbf{X}'_n(t)$ is only a feasible solution. Rearranging the right-hand side of (62), we obtain

$$\begin{aligned} \Phi_1(t) &\leq \sum_{n \in \mathcal{N}} \sum_{f \in \mathcal{F}} (\tilde{w}_{n,f}(t) - w_{n,f}(t)) X_{n,f}^c(t) \\ &\quad + \sum_{n \in \mathcal{N}} \sum_{f \in \mathcal{F}} (w_{n,f}(t) - \tilde{w}_{n,f}(t)) X'_{n,f}(t). \end{aligned} \quad (63)$$

By (33) and (50), we have

$$\begin{aligned} & \tilde{w}_{n,f}(t) - w_{n,f}(t) \\ &= L_f (V \tilde{d}_{n,f}(t) - \alpha Q_n(t)) - L_f (V d_{n,f} - \alpha Q_n(t)) \\ &= V L_f (\tilde{d}_{n,f}(t) - d_{n,f}). \end{aligned} \quad (64)$$

Substituting (64) into (63), we obtain

$$\begin{aligned} \Phi_1(t) &\leq \sum_{n \in \mathcal{N}} \sum_{f \in \mathcal{F}} V L_f (\tilde{d}_{n,f}(t) - d_{n,f}) X_{n,f}^c(t) \\ &\quad + \sum_{n \in \mathcal{N}} \sum_{f \in \mathcal{F}} V L_f (d_{n,f} - \tilde{d}_{n,f}(t)) X'_{n,f}(t). \end{aligned} \quad (65)$$

Next, we define

$$\Phi_2(t) \triangleq \sum_{n \in \mathcal{N}} \sum_{f \in \mathcal{F}} L_f (\tilde{d}_{n,f}(t) - d_{n,f}) X_{n,f}^c(t) \quad (66)$$

and

$$\Phi_3(t) \triangleq \sum_{n \in \mathcal{N}} \sum_{f \in \mathcal{F}} L_f (d_{n,f} - \tilde{d}_{n,f}(t)) X'_{n,f}(t). \quad (67)$$

Then the upper bound of $\Phi_1(t)$ in (65) can be rewritten as

$$\Phi_1(t) \leq V (\Phi_2(t) + \Phi_3(t)). \quad (68)$$

In the following subsections, we obtain the upper bounds of $\Phi_2(t)$ and $\Phi_3(t)$ respectively to bound $\Phi_1(t)$.

B. Bounding $\Phi_2(t)$

To derive the upper bound of $\Phi_2(t)$, we define the event $G_{n,f}(t) \triangleq \{\tilde{d}_{n,f}(t) \geq d_{n,f}\}$ for each $n \in \mathcal{N}$ and $f \in \mathcal{F}$. Then we have

$$\begin{aligned} \Phi_2(t) &= \sum_{n \in \mathcal{N}} \sum_{f \in \mathcal{F}} L_f (\tilde{d}_{n,f}(t) - d_{n,f}) X_{n,f}^c(t) \\ &\quad \cdot (\mathbf{1}\{G_{n,f}(t)\} + \mathbf{1}\{G_{n,f}^c(t)\}) \\ &= \sum_{n \in \mathcal{N}} \sum_{f \in \mathcal{F}} L_f (\tilde{d}_{n,f}(t) - d_{n,f}) X_{n,f}^c(t) \mathbf{1}\{G_{n,f}(t)\} \\ &\quad + \sum_{n \in \mathcal{N}} \sum_{f \in \mathcal{F}} L_f (\tilde{d}_{n,f}(t) - d_{n,f}) X_{n,f}^c(t) \mathbf{1}\{G_{n,f}^c(t)\} \\ &\leq \sum_{n \in \mathcal{N}} \sum_{f \in \mathcal{F}} L_f (\tilde{d}_{n,f}(t) - d_{n,f}) X_{n,f}^c(t) \mathbf{1}\{G_{n,f}(t)\}. \end{aligned} \quad (69)$$

The last inequality holds since when event $G_{n,f}^c(t)$ occurs, we have $\tilde{d}_{n,f}(t) < d_{n,f}$ and $(\tilde{d}_{n,f}(t) - d_{n,f}) \mathbf{1}\{G_{n,f}^c(t)\} < 0$. Next, we define

$$\phi_{2,n,f}(t) \triangleq (\tilde{d}_{n,f}(t) - d_{n,f}) X_{n,f}^c(t) \mathbf{1}\{G_{n,f}(t)\}. \quad (70)$$

Then we rewrite the upper bound of $\Phi_2(t)$ in (69) as

$$\Phi_2(t) \leq \sum_{n \in \mathcal{N}} \sum_{f \in \mathcal{F}} L_f \phi_{2,n,f}(t). \quad (71)$$

Let $t_{n,f}^{(1)}$ be the index of the first time slot in which file f is cached on EFS n . We define event $U_{n,f}(t) \triangleq \{\tilde{d}_{n,f}(t) - d_{n,f} > K_n \sqrt{\frac{3 \log t}{2(h_{n,f}(t) + H_{n,f})}}\}$ for each $n \in \mathcal{N}$ and $f \in \mathcal{F}$. Summing $\phi_{2,n,f}(t)$ over time slots $\{0, 1, \dots, T-1\}$, it turns out that

$$\begin{aligned} & \sum_{t=0}^{T-1} \phi_{2,n,f}(t) \\ &= \sum_{t=0}^{T-1} (\tilde{d}_{n,f}(t) - d_{n,f}) X_{n,f}^c(t) \mathbf{1}\{G_{n,f}(t)\} \\ &\leq K_n X_{n,f}^c(t) \\ &\quad + \sum_{t=t_{n,f}^{(1)}+1}^{T-1} (\tilde{d}_{n,f}(t) - d_{n,f}) X_{n,f}^c(t) \mathbf{1}\{G_{n,f}(t)\} \\ &= K_n X_{n,f}^c(t) \\ &\quad + \sum_{t=t_{n,f}^{(1)}+1}^{T-1} (\tilde{d}_{n,f}(t) - d_{n,f}) X_{n,f}^c(t) \mathbf{1}\{G_{n,f}(t)\} \\ &\quad \cdot (\mathbf{1}\{U_{n,f}(t)\} + \mathbf{1}\{U_{n,f}^c(t)\}) \\ &= K_n X_{n,f}^c(t) \\ &\quad + \sum_{t=t_{n,f}^{(1)}+1}^{T-1} (\tilde{d}_{n,f}(t) - d_{n,f}) X_{n,f}^c(t) \\ &\quad \cdot \mathbf{1}\{G_{n,f}(t) \cap U_{n,f}(t)\} \\ &\quad + \sum_{t=t_{n,f}^{(1)}+1}^{T-1} (\tilde{d}_{n,f}(t) - d_{n,f}) X_{n,f}^c(t) \\ &\quad \cdot \mathbf{1}\{G_{n,f}(t) \cap U_{n,f}^c(t)\}. \end{aligned} \quad (72)$$

Next, we define

$$\phi_{2,n,f}^{(1)}(t) \triangleq \left(\tilde{d}_{n,f}(t) - d_{n,f} \right) X_{n,f}^c(t) \cdot \mathbb{1} \{G_{n,f}(t) \cap U_{n,f}(t)\} \quad (73)$$

and

$$\phi_{2,n,f}^{(2)}(t) \triangleq \left(\tilde{d}_{n,f}(t) - d_{n,f} \right) X_{n,f}^c(t) \cdot \mathbb{1} \{G_{n,f}(t) \cap U_{n,f}^c(t)\}. \quad (74)$$

Then we rewrite inequality (72) as the following equivalent form:

$$\begin{aligned} \sum_{t=0}^{T-1} \phi_{2,n,f}(t) &\leq K_n X_{n,f}^c(t) \\ &+ \sum_{t=t_{n,f}^{(1)}+1}^{T-1} \phi_{2,n,f}^{(1)}(t) + \sum_{t=t_{n,f}^{(1)}+1}^{T-1} \phi_{2,n,f}^{(2)}(t). \end{aligned} \quad (75)$$

By (75), to bound $\phi_{2,n,f}(t)$, we switch to bounding $\phi_{2,n,f}^{(1)}(t)$ and $\phi_{2,n,f}^{(2)}(t)$. In the following, we derive upper bounds for such two terms, respectively.

First, we bound $\sum_{t=t_{n,f}^{(1)}+1}^{T-1} \phi_{2,n,f}^{(1)}(t)$. According to (73), we have

$$\sum_{t=t_{n,f}^{(1)}+1}^{T-1} \phi_{2,n,f}^{(1)}(t) = \sum_{t=t_{n,f}^{(1)}+1}^{T-1} \left(\tilde{d}_{n,f}(t) - d_{n,f} \right) X_{n,f}^c(t) \cdot \mathbb{1} \{G_{n,f}(t) \cap U_{n,f}(t)\}. \quad (76)$$

When event $U_{n,f}(t) = \left\{ \tilde{d}_{n,f}(t) - d_{n,f} > K_n \sqrt{\frac{3 \log t}{2(h_{n,f}(t) + H_{n,f})}} \right\}$ occurs, we consider the following two cases:

- (i) If $\tilde{d}_{n,f}(t) = \min \left\{ \tilde{d}_{n,f}(t) + K_n \sqrt{\frac{3 \log t}{2(h_{n,f}(t) + H_{n,f})}}, K_n \right\} = K_n$, then $\tilde{d}_{n,f}(t) \geq d_{n,f}$, i.e., event $G_{n,f}(t)$ occurs.
- (ii) If $\tilde{d}_{n,f}(t) = \min \left\{ \tilde{d}_{n,f}(t) + K_n \sqrt{\frac{3 \log t}{2(h_{n,f}(t) + H_{n,f})}}, K_n \right\} = \tilde{d}_{n,f}(t) + K_n \sqrt{\frac{3 \log t}{2(h_{n,f}(t) + H_{n,f})}}$, then event $G_{n,f}(t)$ still occurs, i.e., $\tilde{d}_{n,f}(t) > d_{n,f} + 2K_n \sqrt{\frac{3 \log t}{2(h_{n,f}(t) + H_{n,f})}}$.

Therefore, we have $U_{n,f}(t) \subset G_{n,f}(t)$, or equivalently, $\mathbb{1} \{G_{n,f}(t) \cap U_{n,f}(t)\} = \mathbb{1} \{U_{n,f}(t)\}$. It follows that

$$\begin{aligned} \sum_{t=t_{n,f}^{(1)}+1}^{T-1} \phi_{2,n,f}^{(1)}(t) \\ = \sum_{t=t_{n,f}^{(1)}+1}^{T-1} \left(\tilde{d}_{n,f}(t) - d_{n,f} \right) X_{n,f}^c(t) \mathbb{1} \{U_{n,f}(t)\}. \end{aligned} \quad (77)$$

Since $\tilde{d}_{n,f}(t), d_{n,f} \in [0, K_n]$, we have $\tilde{d}_{n,f}(t) - d_{n,f} \leq K_n$. Then we have

$$\sum_{t=t_{n,f}^{(1)}+1}^{T-1} \phi_{2,n,f}^{(1)}(t) \leq \sum_{t=t_{n,f}^{(1)}+1}^{T-1} K_n X_{n,f}^c(t) \mathbb{1} \{U_{n,f}(t)\}. \quad (78)$$

Taking expectation of (78) at both sides, we have

$$\begin{aligned} &\sum_{t=t_{n,f}^{(1)}+1}^{T-1} \mathbb{E} \left[\phi_{2,n,f}^{(1)}(t) \right] \\ &\leq \sum_{t=t_{n,f}^{(1)}+1}^{T-1} K_n \mathbb{E} [X_{n,f}^c(t)] \Pr \{U_{n,f}(t)\} \\ &= \sum_{t=t_{n,f}^{(1)}+1}^{T-1} K_n \mathbb{E} [X_{n,f}^c(t)] \\ &\cdot \Pr \left\{ \tilde{d}_{n,f}(t) - d_{n,f} > K_n \sqrt{\frac{3 \log t}{2(h_{n,f}(t) + H_{n,f})}} \right\}. \end{aligned} \quad (79)$$

Using the Chernoff-Hoeffding bound [46], we have

$$\begin{aligned} &\Pr \left\{ \tilde{d}_{n,f}(t) - d_{n,f} > K_n \sqrt{\frac{3 \log t}{2(h_{n,f}(t) + H_{n,f})}} \right\} \\ &\leq \exp \left(- \frac{2(h_{n,f}(t) + H_{n,f})^2}{(h_{n,f}(t) + H_{n,f}) K_n^2} \cdot K_n^2 \frac{3 \log t}{2(h_{n,f}(t) + H_{n,f})} \right) \\ &= \exp(-3 \log t) = t^{-3}. \end{aligned} \quad (80)$$

Then it follows that

$$\begin{aligned} &\sum_{n \in \mathcal{N}} \sum_{f \in \mathcal{F}} \sum_{t=t_{n,f}^{(1)}+1}^{T-1} L_f \mathbb{E} \left[\phi_{2,n,f}^{(1)}(t) \right] \\ &\leq \sum_{t=1}^{\infty} \sum_{n \in \mathcal{N}} K_n \mathbb{E} \left[\sum_{f \in \mathcal{F}} L_f X_{n,f}^c(t) \right] t^{-3} \\ &\leq \sum_{t=1}^{\infty} \sum_{n \in \mathcal{N}} K_n M_n t^{-3} \\ &= \sum_{n \in \mathcal{N}} K_n M_n \left(1 + \sum_{t=2}^{\infty} t^{-3} \right) \\ &\leq \sum_{n \in \mathcal{N}} K_n M_n \left(1 + \int_1^{\infty} t^{-3} dt \right) = \frac{3}{2} \sum_{n \in \mathcal{N}} K_n M_n. \end{aligned} \quad (81)$$

Next, we consider the upper bound of $\sum_{t=t_{n,f}^{(1)}+1}^{T-1} \phi_{2,n,f}^{(2)}(t)$. According to (74), we have

$$\sum_{t=t_{n,f}^{(1)}+1}^{T-1} \phi_{2,n,f}^{(2)}(t) = \sum_{t=t_{n,f}^{(1)}+1}^{T-1} \left(\tilde{d}_{n,f}(t) - d_{n,f} \right) X_{n,f}^c(t) \cdot \mathbb{1} \{G_{n,f}(t) \cap U_{n,f}^c(t)\}. \quad (82)$$

When event $U_{n,f}^c(t)$ occurs, we have

$$\begin{aligned} \tilde{d}_{n,f}(t) &= \min \left\{ \tilde{d}_{n,f}(t) + K_n \sqrt{\frac{3 \log t}{2(h_{n,f}(t) + H_{n,f})}}, K_n \right\} \\ &\leq \tilde{d}_{n,f}(t) + K_n \sqrt{\frac{3 \log t}{2(h_{n,f}(t) + H_{n,f})}}, \end{aligned} \quad (83)$$

thus

$$\tilde{d}_{n,f}(t) - d_{n,f} = \left(\tilde{d}_{n,f}(t) - \tilde{d}_{n,f}(t) \right)$$

$$+ (\bar{d}_{n,f}(t) - d_{n,f}) \leq 2K_n \sqrt{\frac{3 \log t}{2(h_{n,f}(t) + H_{n,f})}}. \quad (84)$$

Then by (84) and $X_{n,f}(t) \leq 1$, we have

$$\begin{aligned} & \sum_{t=t_{n,f}^{(1)}+1}^{T-1} \phi_{2,n,f}^{(2)}(t) \\ &= \sum_{t=t_{n,f}^{(1)}+1}^{T-1} 2K_n X_{n,f}^c(t) \sqrt{\frac{3 \log t}{2(h_{n,f}(t) + H_{n,f})}} \\ & \quad \cdot \mathbf{1}\{G_{n,f}(t) \cap U_{n,f}^c(t)\} \\ &\leq \sum_{t=t_{n,f}^{(1)}+1}^{T-1} 2K_n X_{n,f}^c(t) \sqrt{\frac{3 \log t}{2(h_{n,f}(t) + H_{n,f})}} \\ &\leq \sum_{t=t_{n,f}^{(1)}+1}^{T-1} K_n \sqrt{6 \log T} \frac{X_{n,f}^c(t)}{\sqrt{h_{n,f}(t) + H_{n,f}}}. \end{aligned} \quad (85)$$

Since $h_{n,f}(t) \leq T$, we have

$$\begin{aligned} \frac{1}{\sqrt{h_{n,f}(t) + H_{n,f}}} &= \sqrt{\frac{h_{n,f}(t)}{h_{n,f}(t) + H_{n,f}}} \cdot \frac{1}{\sqrt{h_{n,f}(t)}} \\ &\leq \sqrt{\frac{T}{T + H_{n,f}}} \cdot \frac{1}{\sqrt{h_{n,f}(t)}}. \end{aligned} \quad (86)$$

Then it follows that

$$\sum_{t=t_{n,f}^{(1)}+1}^{T-1} \phi_{2,n,f}^{(2)}(t) \leq \sum_{t=t_{n,f}^{(1)}+1}^{T-1} K_n \sqrt{\frac{6T \log T}{T + H_{n,f}}} \frac{1}{\sqrt{h_{n,f}(t)}}. \quad (87)$$

Let $t_{n,f}^{(i)}$ be the i -th time slot in which file f is cached on EFS n . Then $t_{n,f}^{(h_{n,f}(T))}$ is the time slot in which file f is lastly cached before time slot T . Accordingly, we have

$$\begin{aligned} & \sum_{t=t_{n,f}^{(1)}+1}^{T-1} \frac{1}{\sqrt{h_{n,f}(t)}} = \sum_{i=2}^{h_{n,f}(T)} \frac{1}{\sqrt{h_{n,f}(t_{n,f}^{(i)})}} \\ &= \sum_{i=2}^{h_{n,f}(T)} \frac{1}{\sqrt{i-1}} = \sum_{i=1}^{h_{n,f}(T)-1} \frac{1}{\sqrt{i}} \\ &\leq \int_1^{h_{n,f}(T)} \frac{1}{\sqrt{i}} di = 2 \left(\sqrt{h_{n,f}(T)} - 1 \right) \\ &\leq 2\sqrt{h_{n,f}(T)}. \end{aligned} \quad (88)$$

It follows that

$$\sum_{t=t_{n,f}^{(1)}+1}^{T-1} \phi_{2,n,f}^{(2)}(t) \leq 2K_n \sqrt{\frac{6T \log T}{T + H_{n,f}}} \sqrt{h_{n,f}(T)}. \quad (89)$$

Combining (71), (75), (81) and (89), we have

$$\begin{aligned} & \sum_{t=0}^{T-1} \mathbb{E}[\Phi_2(t)] \leq \sum_{n \in \mathcal{N}} \sum_{f \in \mathcal{F}} L_f \sum_{t=0}^{T-1} \mathbb{E}[\phi_{2,n,f}(t)] \\ &\leq \frac{5}{2} \sum_{n \in \mathcal{N}} K_n M_n \\ & \quad + 2 \sum_{n \in \mathcal{N}} \sum_{f \in \mathcal{F}} L_f K_n \sqrt{\frac{6T \log T}{T + H_{n,f}}} \sqrt{h_{n,f}(T)} \\ &\leq \frac{5}{2} \sum_{n \in \mathcal{N}} K_n M_n \\ & \quad + 2\sqrt{\frac{6T \log T}{T + H_{\min}}} \sum_{n \in \mathcal{N}} K_n \sum_{f \in \mathcal{F}} L_f \sqrt{h_{n,f}(T)}, \end{aligned} \quad (90)$$

where we define a non-negative integer $H_{\min} \triangleq \min_{n,f} H_{n,f}$. The last inequality holds because that $\sum_{f \in \mathcal{F}} L_f X_{n,f}^c(t) \leq M_n$ for each $n \in \mathcal{N}$. On the other hand, by Jensen's inequality, we have

$$\begin{aligned} \sum_{f \in \mathcal{F}} \frac{L_f}{\sum_{f \in \mathcal{F}} L_f} \sqrt{h_{n,f}(T)} &\leq \sqrt{\frac{\sum_{f \in \mathcal{F}} L_f h_{n,f}(T)}{\sum_{f \in \mathcal{F}} L_f}} \\ &\leq \sqrt{\frac{M_n T}{\sum_{f \in \mathcal{F}} L_f}}. \end{aligned} \quad (91)$$

Then it follows that

$$\begin{aligned} \sum_{t=0}^{T-1} \mathbb{E}[\Phi_2(t)] &\leq \frac{5}{2} \sum_{n \in \mathcal{N}} K_n M_n \\ & \quad + 2 \left(\sum_{n \in \mathcal{N}} K_n \sqrt{M_n \sum_{f \in \mathcal{F}} L_f} \right) \sqrt{\frac{6T^2 \log T}{T + H_{\min}}}. \end{aligned} \quad (92)$$

C. Bounding $\Phi_3(t)$

Recall by (67) and $G_{n,f}(t) \triangleq \{\tilde{d}_{n,f}(t) \geq d_{n,f}\}$ that

$$\begin{aligned} \Phi_3(t) &= \sum_{n \in \mathcal{N}} \sum_{f \in \mathcal{F}} L_f \left(d_{n,f} - \tilde{d}_{n,f}(t) \right) X'_{n,f}(t) \\ &= \sum_{n \in \mathcal{N}} \sum_{f \in \mathcal{F}} L_f \left(d_{n,f} - \tilde{d}_{n,f}(t) \right) X'_{n,f}(t) \\ & \quad \cdot \left(\mathbf{1}\{G_{n,f}(t)\} + \mathbf{1}\{G_{n,f}^c(t)\} \right) \\ &\leq \sum_{n \in \mathcal{N}} \sum_{f \in \mathcal{F}} L_f \left(d_{n,f} - \tilde{d}_{n,f}(t) \right) X'_{n,f}(t) \mathbf{1}\{G_{n,f}^c(t)\}. \end{aligned} \quad (93)$$

Then we define

$$\phi_{3,n,f}(t) \triangleq \left(d_{n,f} - \tilde{d}_{n,f}(t) \right) X'_{n,f}(t) \mathbf{1}\{G_{n,f}^c(t)\}, \quad (94)$$

whereby the upper bound of $\Phi_3(t)$ in (93) can be written as

$$\Phi_3(t) \leq \sum_{n \in \mathcal{N}} \sum_{f \in \mathcal{F}} L_f \phi_{3,n,f}(t). \quad (95)$$

Next, we consider the case where $t \leq t_{n,f}^{(1)}$ and the case where $t \geq t_{n,f}^{(1)} + 1$, respectively. When $t \leq t_{n,f}^{(1)}$, we have $\tilde{d}_{n,f}(t) = K_n$. Then the event $G_{n,f}^c(t) = \{\tilde{d}_{n,f}(t) < d_{n,f}\}$ would not occur since $d_{n,f} \leq K_n$. Therefore, $\phi_{3,n,f}(t) = 0$ when $t \leq t_{n,f}^{(1)}$.

When $t \geq t_{n,f}^{(1)} + 1$, suppose that event $G_{n,f}^c(t)$ occurs. Then we have $\bar{d}_{n,f}(t) < d_{n,f} \leq K_n$, which implies that $\tilde{d}_{n,f}(t) = \bar{d}_{n,f}(t) + K_n \sqrt{\frac{3 \log t}{2(h_{n,f}(t) + H_{n,f})}}$. It follows that $d_{n,f} > \bar{d}_{n,f}(t) + K_n \sqrt{\frac{3 \log t}{2(h_{n,f}(t) + H_{n,f})}}$. Hence, we bound $\mathbb{E}[\phi_{3,n,f}(t)]$ as follows:

$$\begin{aligned}
& \mathbb{E}[\phi_{3,n,f}(t)] \\
&= \mathbb{E} \left[\left(d_{n,f} - \bar{d}_{n,f}(t) \right) X'_{n,f}(t) \mathbf{1} \{ G_{n,f}^c(t) \} \right] \\
&\leq \mathbb{E} \left[K_n X'_{n,f}(t) \mathbf{1} \{ G_{n,f}^c(t) \} \right] \\
&= K_n X'_{n,f}(t) \mathbb{E} \left[\mathbf{1} \{ G_{n,f}^c(t) \} \right] \\
&= K_n X'_{n,f}(t) \Pr \{ G_{n,f}^c(t) \} \\
&\leq K_n X'_{n,f}(t) \\
&\quad \cdot \Pr \left\{ d_{n,f} > \bar{d}_{n,f}(t) + K_n \sqrt{\frac{3 \log t}{2(h_{n,f}(t) + H_{n,f})}} \right\}.
\end{aligned} \tag{96}$$

By Chernoff-Hoeffding bound, we have

$$\begin{aligned}
& \Pr \left\{ d_{n,f} > \bar{d}_{n,f}(t) + K_n \sqrt{\frac{3 \log t}{2(h_{n,f}(t) + H_{n,f})}} \right\} \\
&= \Pr \left\{ \bar{d}_{n,f}(t) < d_{n,f} - K_n \sqrt{\frac{3 \log t}{2(h_{n,f}(t) + H_{n,f})}} \right\} \\
&\leq \exp(-3 \log t) = t^{-3}.
\end{aligned} \tag{97}$$

Hence, we have

$$\mathbb{E}[\phi_{3,n,f}(t)] \leq K_n X'_{n,f}(t) t^{-3}. \tag{98}$$

Based on the above inequality, we have

$$\begin{aligned}
& \sum_{t=0}^{T-1} \sum_{f \in \mathcal{F}} L_f \mathbb{E}[\phi_{3,n,f}(t)] \\
&\leq K_n \sum_{t=t_{n,f}^{(1)}+1}^{T-1} \sum_{f \in \mathcal{F}} L_f X'_{n,f}(t) t^{-3} \\
&\leq K_n \sum_{t=t_{n,f}^{(1)}+1}^{T-1} M_n t^{-3},
\end{aligned} \tag{99}$$

where the last inequality holds because $\sum_{f \in \mathcal{F}} L_f X'_{n,f}(t) \leq M_n$. Then by (99), it follows that

$$\begin{aligned}
& \sum_{t=0}^{T-1} \sum_{f \in \mathcal{F}} L_f \mathbb{E}[\phi_{3,n,f}(t)] \\
&\leq K_n M_n \sum_{t=t_{n,f}^{(1)}+1}^{T-1} t^{-3} \leq K_n M_n \sum_{t=1}^{\infty} t^{-3} \\
&\leq K_n M_n \left(1 + \sum_{t=2}^{\infty} t^{-3} \right) \\
&\leq K_n M_n \left(1 + \int_1^{\infty} t^{-3} dt \right) = \frac{3}{2} K_n M_n.
\end{aligned} \tag{100}$$

By (95) and (100), we have

$$\begin{aligned}
\sum_{t=0}^{T-1} \mathbb{E}[\Phi_3(t)] &\leq \sum_{n \in \mathcal{N}} \sum_{t=0}^{T-1} \sum_{f \in \mathcal{F}} L_f \mathbb{E}[\phi_{3,n,f}(t)] \\
&\leq \sum_{n \in \mathcal{N}} \frac{3}{2} K_n M_n.
\end{aligned} \tag{101}$$

Combining (68), (92) and (101), we obtain

$$\begin{aligned}
& \sum_{t=0}^{T-1} \mathbb{E}[\Phi_1(t)] \\
&\leq V \left(\sum_{t=0}^{T-1} \mathbb{E}[\Phi_2(t)] + \sum_{t=0}^{T-1} \mathbb{E}[\Phi_3(t)] \right) \\
&\leq 4V \sum_{n \in \mathcal{N}} K_n M_n \\
&\quad + 2V \left(\sum_{n \in \mathcal{N}} K_n \sqrt{M_n \sum_{f \in \mathcal{F}} L_f} \right) \sqrt{\frac{6T^2 \log T}{T + H_{\min}}}.
\end{aligned} \tag{102}$$

Substituting (102) into (59), we obtain a regret bound as follows:

$$\begin{aligned}
Reg(T) &\leq \frac{B}{V} + \frac{4 \sum_{n \in \mathcal{N}} K_n M_n}{T} \\
&\quad + 2 \left(\sum_{n \in \mathcal{N}} K_n \sqrt{M_n \sum_{f \in \mathcal{F}} L_f} \right) \sqrt{\frac{6 \log T}{T + H_{\min}}},
\end{aligned} \tag{103}$$

where $B = \frac{1}{2} \sum_{n \in \mathcal{N}} (b_n^2 + \alpha^2 M_n^2)$ and $H_{\min} = \min_{n,f} H_{n,f}$. \blacksquare